NASA TECHNICAL NOTE

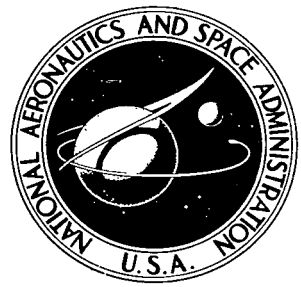

NASA TN D-4489

NASA TN D-4489

LARGE-SCALE WIND-TUNNEL TESTS OF AN AIRPLANE MODEL WITH TWO PROPELLERS AND ROTATING CYLINDER FLAPS

by James A. Weiberg and Berl Gamse

Ames Research Center
Moffett Field, Calif.

NATIONAL AERONAUTICS AND SPACE ADMINISTRATION • WASHINGTON, D. C. • MARCH 1968

LARGE-SCALE WIND-TUNNEL TESTS OF AN AIRPLANE MODEL WITH TWO PROPELLERS AND ROTATING CYLINDER FLAPS

By James A. Weiberg and Berl Gamse

Ames Research Center
Moffett Field, Calif.

NATIONAL AERONAUTICS AND SPACE ADMINISTRATION

For sale by the Clearinghouse for Federal Scientific and Technical Information
Springfield, Virginia 22151 – CFSTI price $3.00

LARGE-SCALE WIND-TUNNEL TESTS OF AN AIRPLANE MODEL WITH TWO PROPELLERS AND ROTATING CYLINDER FLAPS

By James A. Weiberg and Berl Gamse

Ames Research Center

SUMMARY

Wind-tunnel tests were made of a model of a twin turbo-propeller airplane with rotating cylinder flaps. The model had a straight untapered wing of aspect ratio 3.57 equipped with end plates. Cylinder rotation provided a lift coefficient increment of 2.0 and a maximum lift coefficient of 4.0 with 60° flap deflection and zero propeller thrust. A maximum lift coefficient of 9.1 was obtained with a thrust coefficient of 4. The cylinder rotational speed required varied with flap deflection and was independent of angle of attack and slipstream velocity. For a flap deflection of 60° and a free-stream velocity of 40 knots, the cylinder power required was approximately 0.7 horsepower per foot of cylinder length.

INTRODUCTION

On the basis of the encouraging results (ref. 1) of small-scale tests, an investigation was made of the rotating cylinder flap principle applied to a large three-dimensional model. These tests were made to determine the rotating cylinder flap effectiveness and power requirements as affected by free-stream velocity, propeller slipstream, cylinder peripheral speed, and ground proximity. The investigation included the effects of flap hinge line location on flap effectiveness, wing pitching moments, and flap hinge moments, and the effectiveness of slats and spoilers in conjunction with the rotating cylinder flap.

The tests were made in the Ames 40- by 80-Foot Wind Tunnel.

NOTATION

b	wing span, 25 ft
C_D	drag coefficient, $\frac{D}{qS}$
C_{h_f}	flap hinge-moment coefficient, $\frac{HM}{qS_f c_f}$
C_L	lift coefficient, $\frac{L}{qS}$

C_l rolling-moment coefficient, $\frac{L}{qSb}$

C_m pitching-moment coefficient, $\frac{M}{qSc}$

C_n yawing-moment coefficient, $\frac{N}{qSb}$

C_T thrust coefficient, $\frac{T}{\rho n^2 D^4}$

C_Y side-force coefficient, $\frac{Y}{qS}$

c wing chord, 7 ft

c_f flap chord, 2.75 ft

D drag, lb, and propeller diameter, ft

HM flap hinge moment, ft-lb

h height of wing chord above ground plane ($\alpha = 0$), ft, and height of spoiler, ft

J propeller advance ratio, $\frac{V}{nD}$

L lift, lb, and rolling moment, ft-lb

M pitching moment about 0.25c, ft-lb

N yawing moment, ft-lb

n propeller angular velocity, rps

q free-stream dynamic pressure, psf

S wing area, 175 sq ft

S_f flap area, 60.5 sq ft

T thrust, lb

T_c' thrust coefficient, $\frac{T}{qS}$

U peripheral velocity, fps

V free-stream velocity, fps

Y side force, lb

α wing angle of attack, deg

β blade angle at 0.75R, deg

γ descent angle, deg

δ_a aileron deflection, deg

δ_A flapevator deflection, deg

δ_f flap deflection, deg

θ turning angle, deg

ρ mass density of air, slugs/cu ft

MODEL

The model for these tests represented a twin-engine turbo-propeller airplane and is shown mounted in the wind tunnel in figure 1. For structural reasons, the model was tested without a tail. The geometry and dimensions are given in figure 2(a). Details of the flap, wing leading-edge slat, spoilers, and end plates are shown in figures 1 and 2.

A 10.9-inch-diameter machined aluminum cylinder (0.25-inch wall) was built into the leading edge of the flap (fig. 2(b)). The cylinder was in four segments, each 65.1 inches long and driven by an electric motor. The cylinders had 18.2-inch-diameter disks on the ends at the wing tips and fuselage. The cylinders were separated 0.25 inch and fitted with 13.4-inch-diameter disks at mid-semispan. The flap included a slotted aft segment called a flapevator with a chord 19 percent of the wing chord. The flap could be deflected about various hinge positions. The two positions tested are shown in figure 2(b).

The model had 2 three-bladed propellers. The geometric blade characteristics of these propellers are shown in figure 2(d). The blade angle at 0.75 blade radius was 18°. The majority of the data were obtained with the inboard blade of both propellers rotated downward as shown in figure 2(a) and, unless noted, the data presented are with this rotation.

The model was mounted on adjustable height support struts above a simulated ground plane that was 3 feet above the tunnel floor. For the ground effect tests, the model was positioned so that the wing chord ($\alpha = 0$) was 9.73 feet ($h/c = 1.39$) above the simulated ground. For all other tests, the model was 15.13 feet ($h/c = 2.16$) above the ground plane.

TESTS AND CORRECTIONS

Tests were made at free-stream dynamic pressures of 2.6 and 5 psf (R = 2.1 and 2.9 million). (Unless noted on the figures, the data are for 2.6 psf.) The data from these tests, presented in the figures, include the direct propeller forces as well as the aerodynamic forces. The propeller

thrust characteristics are given in figure 2(e). Forces and moments are about the wind axis for a moment center at 0.25 chord.

Corrections to the lift, drag, and pitching moment were made for the tare due to the model support struts. Tunnel wall corrections were not applied because the relative size of the model and the wind tunnel was within the boundaries indicated in reference 2 for best correlation between wind-tunnel and flight-test results. The conventional tunnel wall corrections are

$$\alpha = \alpha_u + 0.51\ C_L$$

$$C_D = C_{D_u} + 0.0089\ C_L^2$$

where the subscript u stands for uncorrected data.

RESULTS

An index to the figures is presented in table I.

The effect of cylinder rotation on lift is shown in figures 3 and 4. The cylinder rpm and power required for the U/V values in figure 3 are given in figures 5 and 6. Power to the cylinders was determined from measurements of electrical power input to the drive motors and corrected for a motor efficiency of 92 percent obtained from a dynamometer calibration of the motors.

The effect of angle of attack on the longitudinal characteristics of the model with the flap deflected about hinge 1 (fig. 2(b)) and with constant cylinder rpm are shown in figures 7, 8, and 9.[1] The effect of end plates, slats, and propeller rotation are shown in figure 10. The effect of height above a ground plane is shown in figure 11. A comparison with results obtained on the model with mechanical flaps (fig. 12) is shown in figure 13.

Aerodynamic characteristics of the model with the flaps deflected about hinge 2 (fig. 2(b)) are shown in figures 14 and 15. Comparisons with the results for hinge 1 are shown in figure 16. The effects of extending the flap chord (fig. 2(c)) are shown in figures 17 and 18. These data are based on the area and chord with the extension.

Lateral control characteristics are shown in figure 19.

Flap hinge moments obtained from strain-gage measurements on the flap actuator arms are shown in figure 20.

---

[1]Because of the difficulty in maintaining a constant thrust coefficient of 8, the data were crossplotted against thrust coefficient to obtain the curves for $T_c' = 8$ and are presented without data points.

DISCUSSION

With the cylinder rotating, airflow on the flap was strongly attached and was insensitive to exterior effects such as a slat, propeller slipstream, or surface disturbances ahead of the cylinder.

Flap Effectiveness

The effect of cylinder speed on lift is shown in figure 3. Cylinder speed is expressed as a ratio of cylinder surface speed to free-stream velocity U/V.

At low velocity ratios U/V, the flow over the surface of the flap is separated. As cylinder speed is increased, the separated area on the flap is reduced and at the knee of the curves in figure 3 the flow is completely attached. Further increases in cylinder speed increased lift only slightly. As shown in figure 3, the velocity ratio U/V for attached flow varied with flap deflection and was independent of angle of attack, propeller slipstream effects, and free-stream velocity.

Flap lift increments computed by the simple flap theory of reference 3 are compared with the measured values in figure 4. The measured values were slightly higher than the computed values and were the same for the flap pivoted about hinge 1 or 2. Deflecting the flapevator (aft flap) provided additional lift. Lift increments for the mechanical flap[2] are also shown in figure 4 and were approximately 0.7 or less of the computed values. The rotating cylinder flap also provided higher turning effectiveness and thrust recovery in hover (fig. 13(b)) than the mechanical flap.

Power Requirements

The power required to rotate the cylinders is presented as a function of rpm in figure 6. This figure shows that power was nearly proportional to the cube of rpm and independent of airspeed (within the limits of the test) and flap deflection (amount of exposed cylinder). Thus, for a constant flap deflection (and hence constant U/V), cylinder power required for attached flow would be proportional to the cube of the airspeed. For 60° flap deflection at 40 knots, approximately 0.7 hp per foot of cylinder length was required for flow attachment, but at 80 knots the power required would be nearly 6 hp per foot.

Results are presented in reference 4 of a blowing boundary-layer-control (BLC) flap on an aspect ratio 5.5 wing. The lift effectiveness and power requirements of this flap are compared with the RCF in the following table. Power is in horsepower per foot of length of either the cylinder or the blowing flap.

---

[2]The mechanical flap and rotating cylinder flap geometry can be compared from figures 2 and 12.

	δ_f, deg	ΔC_{L_f}		$C_{L_{max}}$	hp/ft	
		Theory	Experiment		V = 40k	V = 80k
RCF	60/18	2.7	3.2	4.0	0.74	6.0
Blowing flap	80	3.0	2.8	3.7	3.5[a]	14.0[a]

[a]Isentropic power required for a duct pressure ratio of 2.0.

For approximately the same lift, the RCF required less power than the blowing BLC flap.

Longitudinal Characteristics

Flap lift increment was constant up to maximum lift coefficient ($C_{L_{max}}$). In the following table the $C_{L_{max}}$ obtained with the RCF are compared with values for the mechanical flap.

	δ_f, deg	δ_A, deg	Hinge	$C_{L_{max}}$	
				Power off, $T_c' = 0$	Power on, $T_c' = 4$
RCF	40	10	1	3.0	7.9
	60	18[a]	1	4.0	9.1
	40	10	2	3.2	8.3
	60	18	2	3.5	8.3
Mechanical flap	40	10	-	2.5	7.2
	60	30[a]	-	3.0	7.5

[a]Leading-edge slats on.

Maximum lift coefficients were higher when the propeller blades were down-going next to the fuselage than when they rotated in the opposite direction (fig. 10(a)). Leading-edge slats increased power-off ($T_c' = 0$) maximum lift but had no effect with power on (fig. 10(b)).

Pitching moments (tail off) were relatively small for all flap deflections and thrust coefficients when the flap hinge was on the wing upper surface (hinge 2, fig. 2(b)). The moments are compared with those for the mechanical flap in the following table.

	δ_f, deg	δ_A, deg	Hinge	C_m at $\alpha = 12^\circ$		
				$T_c' = 0$	4	8
RCF	40	10	1	-0.25	-0.25	
	60	18[a]	1	-.32	-.65	-1.2
	70	18[a]	1	-.30	-.60	-1.3
	40	10	2	-.14	0	
	60	18	2	-.10	-.13	
Mechanical flap	40	10	-	-.23	-.73	
	60	30	-	-.20	-.88	-1.55

[a]Leading-edge slats on.

The smaller pitching moments with hinge 2 would require smaller tail size, loads, and deflections for trim; the lower negative tail loads would result in higher total airplane lift. The strongly attached flow on the RCF should alleviate tail buffeting.

The rotating cylinder flap provided higher lift with corresponding higher drag than the mechanical flap (fig. 13(a)). A descent angle capability of 20° at α for maximum lift ($T_c' = 4$) was indicated with 70/18 RCF deflection (fig. 9(d)). The steeper descent and higher C_L (slower touchdown speed) would result in shorter landing approach and ground roll distances.

Lower wing pitching moments and flap hinge moments for approximately the same maximum lift were obtained with the flap hinge line on the wing upper surface rather than on the lower surface (figs. 16 and 20).

A 0.1 chord flap extension increased drag at a given lift without changing pitching moment (fig. 18). With the chord extension, maximum lift coefficient was less but the lift coefficient at low angles of attack was higher.

Lateral Control

The lateral control effectiveness of ailerons and spoilers with the RCF and with the mechanical flap are compared in the following table. The outboard partial span flapevators were differentially deflected $\pm 10^\circ$ to act as ailerons. The geometry of the ailerons and spoilers is shown in figures 2 and 12.

		δ_f, deg	δ_A, deg	ΔC_l ($\alpha = 8^\circ$)		ΔC_n ($\alpha = 8^\circ$)	
				$T_c' = 0$	$T_c' = 4$	$T_c' = 0$	$T_c' = 4$
RCF							
Ailerons	$\delta_a = \pm 10^\circ$	40	10	0.045	0.103	-0.026	-0.106
Flap spoilers	$\frac{h}{c} = 0.15$	70	18	.13	.200	-.086	-.156
Mechanical flap							
Ailerons	$\delta_a = \pm 10^\circ$	20	0	.028	.083	0	-.016
Wing spoilers	$\frac{h}{c} = 0.077$	60	30	.086	.105	-.030	-.052

Because of higher flap lift, rolling moments were greater with the flap-mounted spoilers with the RCF than with the wing mounted spoilers with the mechanical flap. However, higher adverse yaw accompanied these higher rolling moments.

CONCLUDING REMARKS

This study has shown that the rotating cylinder flap can be an effective and efficient high lift device in the operating regions investigated. Cylinder rotational speed required is a direct function of airspeed and an inverse function of airfoil thickness (cylinder diameter limitation). The power required is proportional to the cube of the velocity; therefore, the mechanical requirements for rotating cylinder flaps will rapidly become more stringent if airspeed is increased, and detailed design efforts will be required to establish the feasibility of the device when used on aircraft with high approach speeds. However, the power requirements are less than for a comparable blowing flap BLC system. Proper choice of hinge line about which the rotating cylinder flap pivots can result in substantially lower pitching moments and flap hinge moments than those for a conventional mechanical flap.

Ames Research Center
National Aeronautics and Space Administration
Moffett Field, Calif., 94035, Nov. 27, 1967
721-01-00-12-00-21

REFERENCES

1. Alvarez-Calderon, Alberto; and Arnold, Frank R.: A Study of the Aerodynamic Characteristics of a High-Lift Device Based on a Rotating Cylinder and Flap. Stanford University Technical Report RCF-1, 1961.

2. Cook, Woodrow L.; and Hickey, David H.: Comparison of Wind-Tunnel and Flight-Test Aerodynamic Data in the Transition-Flight Speed Range for Five V/STOL Aircraft. NASA SP-116, 1966, pp. 447-467.

3. DeYoung, John: Theoretical Symmetric Span Loading Due to Flap Deflection for Wings of Arbitrary Plan Form at Subsonic Speeds. NACA TN 1071, 1952.

4. Weiberg, James A.; and Holzhauser, Curt A.: Large-Scale Wind-Tunnel Tests of an Airplane Model With an Unswept, Tilt Wing of Aspect Ratio 5.5, and With Four Propellers and Blowing Flaps. NASA TN D-1034, 1961.

TABLE I.- FIGURE INDEX

Figure	Data	δ_f, deg	δ_A, deg	U/V (nom.)	Hinge	q	Slats	End plates	T_c' (nom.)	Propeller rotation
Effect of cylinder rotation										
3(a)	C_L vs. U/V	40	10	Variable	1	2.6	Off	Off	0	
3(b)	↓	60	0,18	↓	1,2	2.6,5	-	-	0,4	↓
3(c)		70	18		1	2.6	On	On	4	
Longitudinal characteristics, hinge 1										
7	C_D, α, C_m, vs. C_L	60	18	0	1	2.6	Off	Off	0,4,8	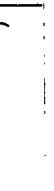
8(a)	↓	40	0	5.0	↓	↓	Off	On	0,4	↓
8(b)		60	0	6.6			Off	Off	0,4	
8(c)		70	0	6.6			On	On	0,4	
9(a)		40	10	5.0			Off	↓	0,4	
9(b)		60	18	6.6			Off		0,4,8	
9(c)		60	18	↓			On		0,4,8	
9(d)		70	18				On		0,4,8	
	Effect of:									
10(a)	δ_A and propeller rotation	60	-				Off	Off	4	-
10(b)	End plates and slats	60	18				-	-	0,4	
11	Ground height	70	18				On	On	0,4	↓
13	Comparison with mechanical flap	60	-	-	↓	↓	-	-	0,4	
Longitudinal characteristics, hinge 2										
14(a)	C_D, α, C_m vs. C_L	40	0	5.0	2	2.6	Off	On	0,4	
14(b)	↓	60	0	6.6	↓	↓	↓	↓	↓	↓
15(a)		40	10	5.0						
15(b)		60	18	6.6						
16(a)	Comparison with hinge 1	60	18	6.6	1,2					
16(b)	Comparison with hinge 1[a]	60	18	6.6	1,2	↓	On	↓	↓	↓
Longitudinal characteristics with flap chord extension										
17(a)	C_D, α, C_m, vs. C_L	60	18	6.6	1	2.6	On	On	0,4	
17(b)	↓	↓	↓	↓	2	↓	On	↓	↓	↓
17(c)					2		Off			
18(a)	Comparison without extension				1		On			
18(b)	Comparison without extension	↓	↓	↓	2	↓	Off	↓	↓	↓
Lateral control effectiveness										
19(a)	Ailerons	40	10	5.0	1	2.6	Off	On	0,4	
19(b)	Spoiler	70	18	6.6	1	2.6	On	On	0,4	↓
Flap hinge moments										
20	C_{h_f} vs. α	40	10	5.0	1,2	2.6	Off	On	0,4	
	↓	60	18	6.6	1,2	2.6	Off	On	0,4	↓

[a] With flap chord extension.

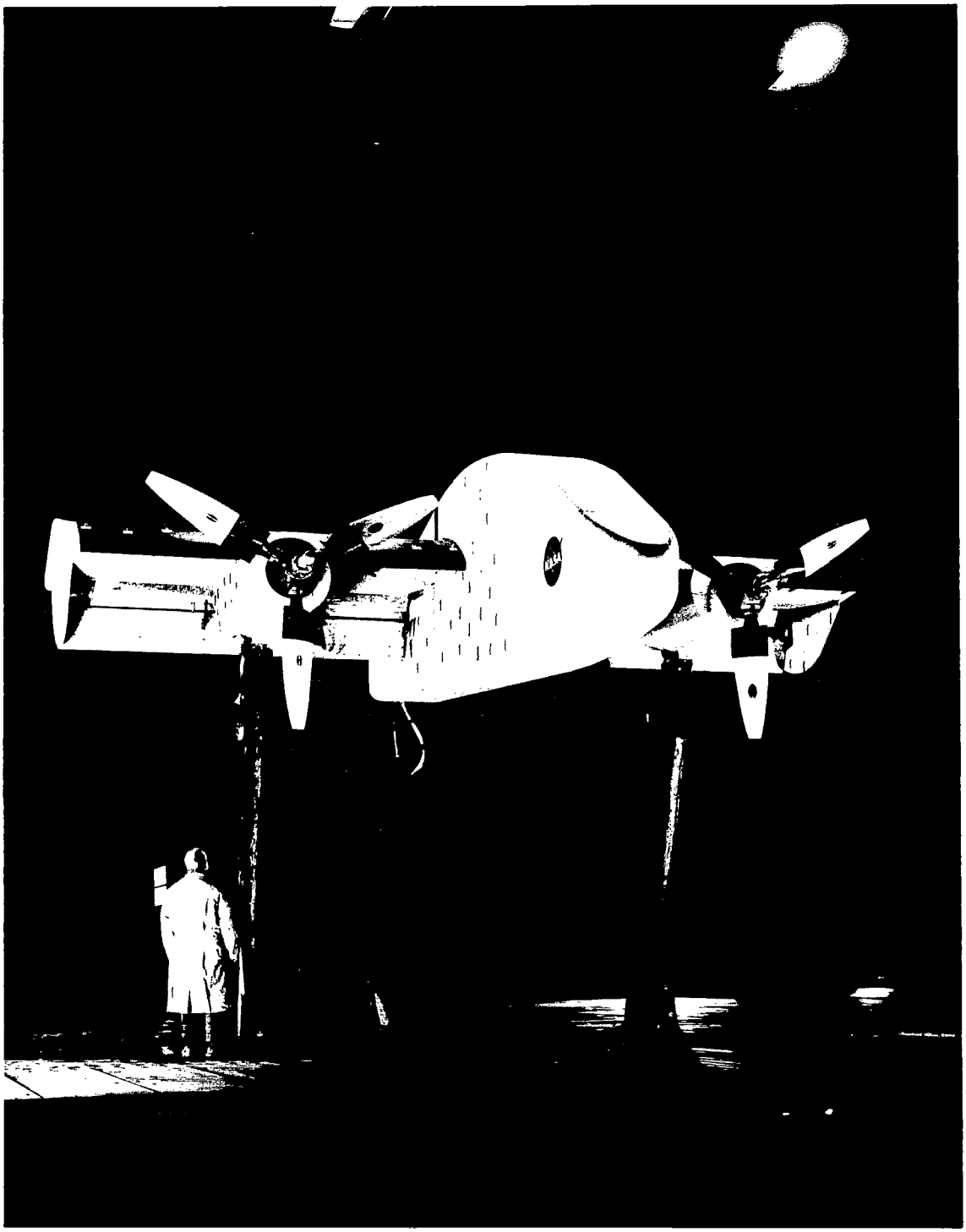

(a) The model with slats on and flaps deflected. A-36430

Figure 1.- The model mounted in the wind tunnel.

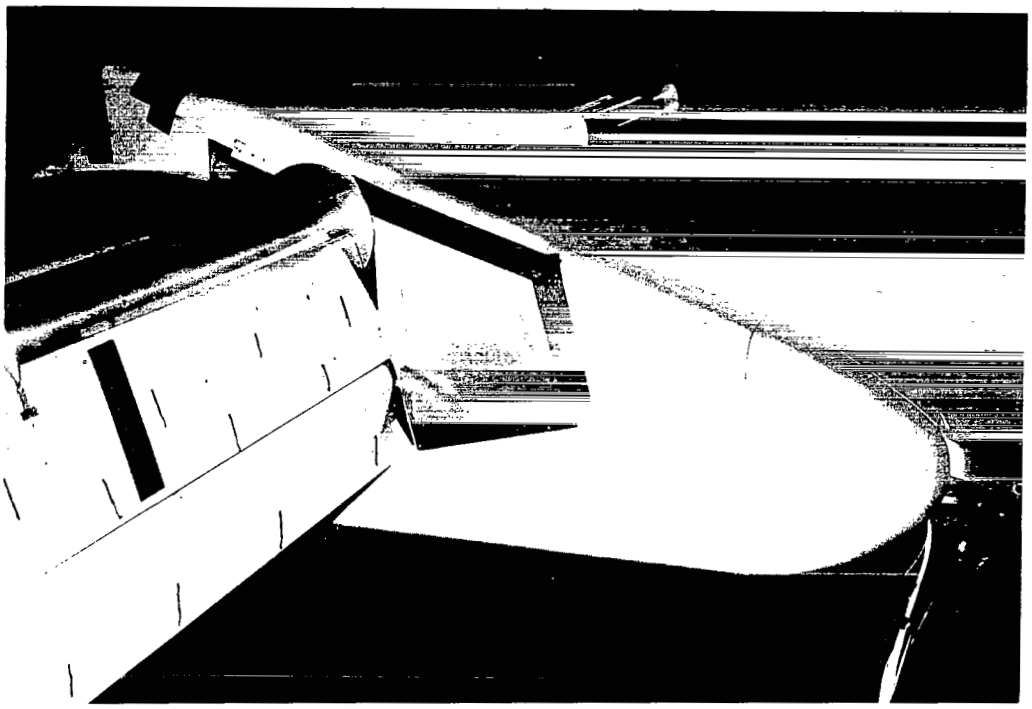

(b) Detail of cylinder. A-36429

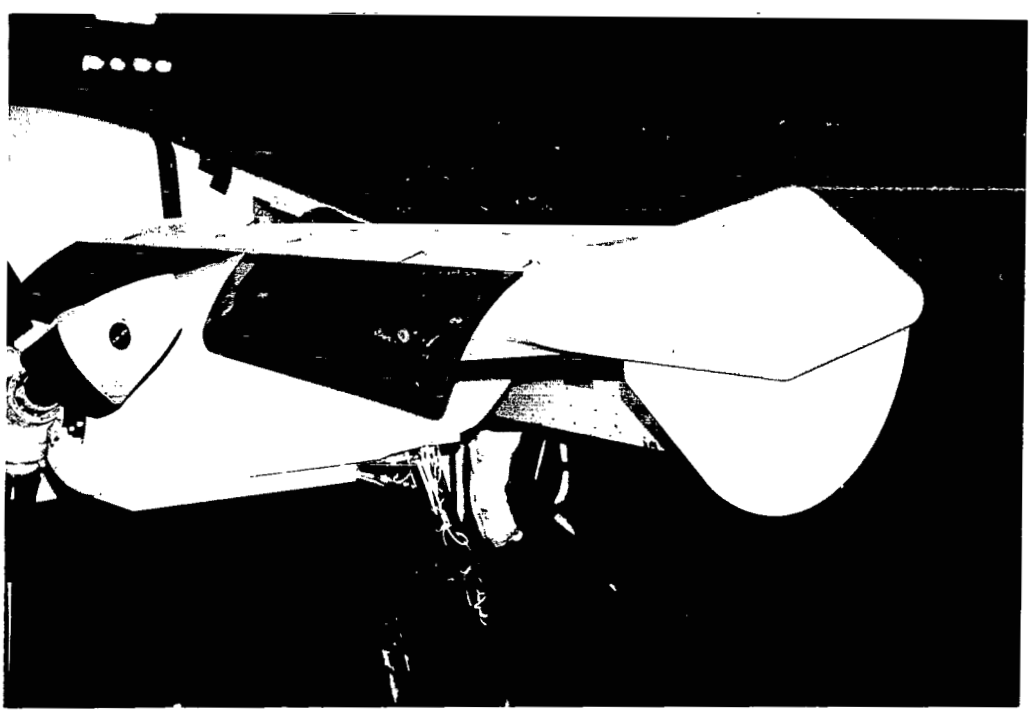

(c) Detail of slat and end plate. A-36428

Figure 1.- Concluded.

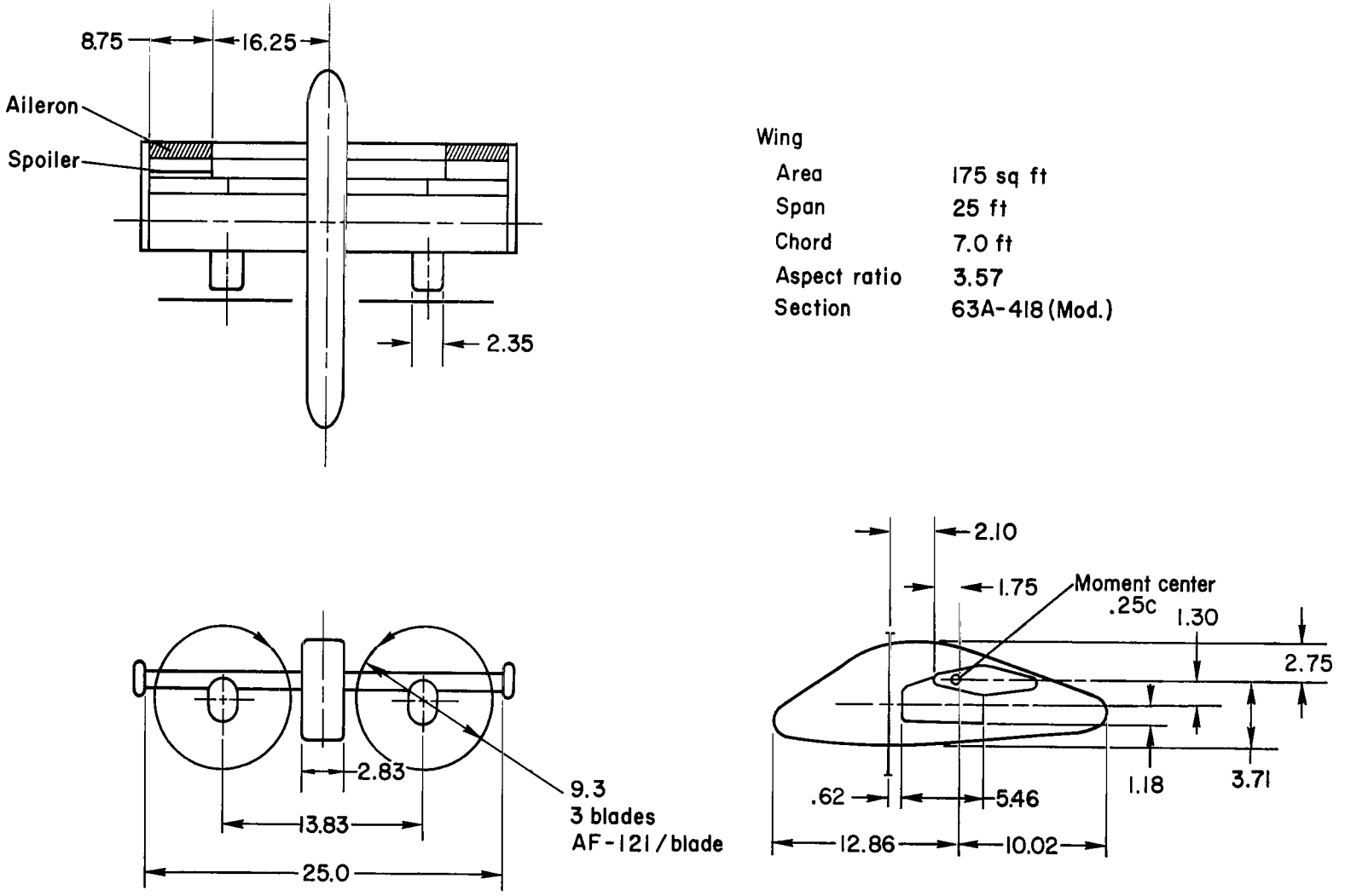

(a) General dimensions (feet).

Figure 2.- Geometry of the model.

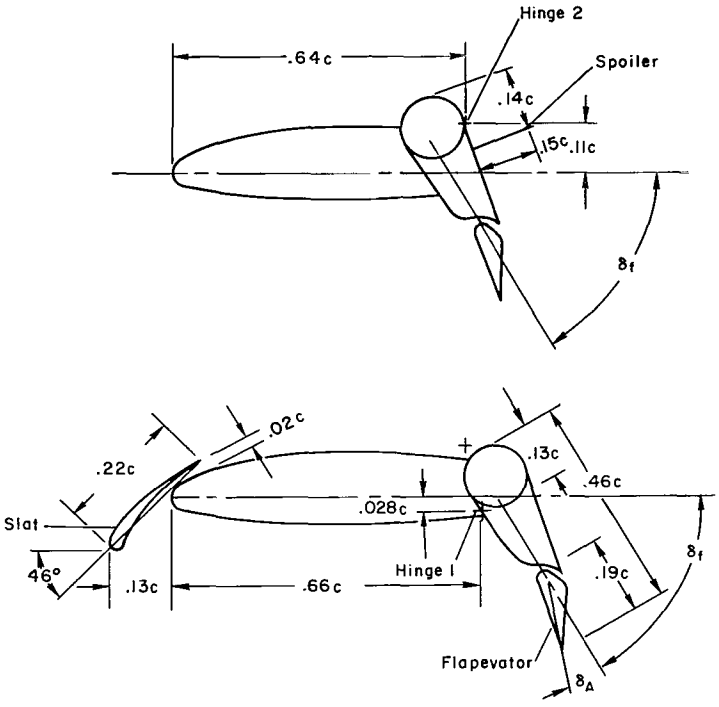

(b) Slat and flap geometry.

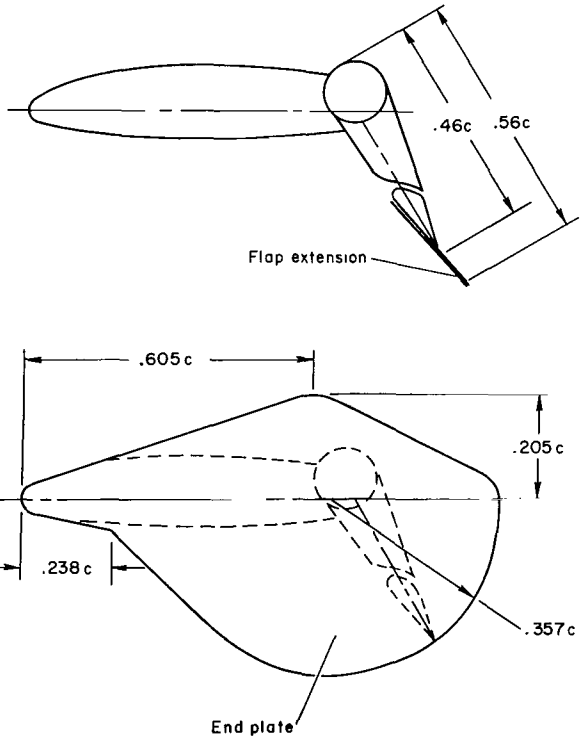

(c) Flap extension and end plate.

Figure 2.- Continued.

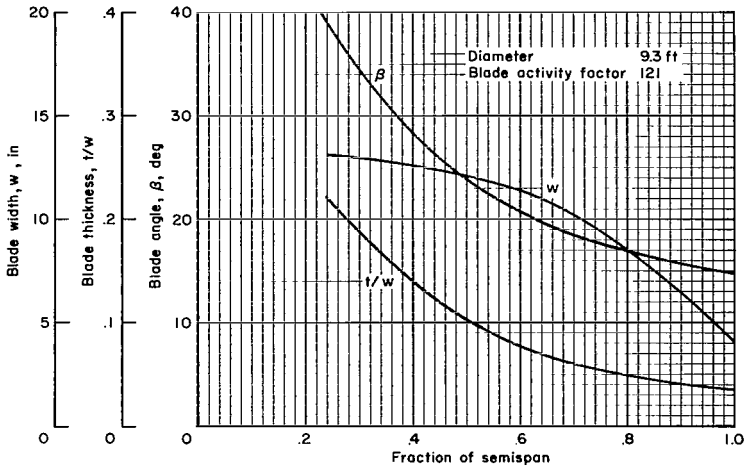

(d) Propeller blade form curves.

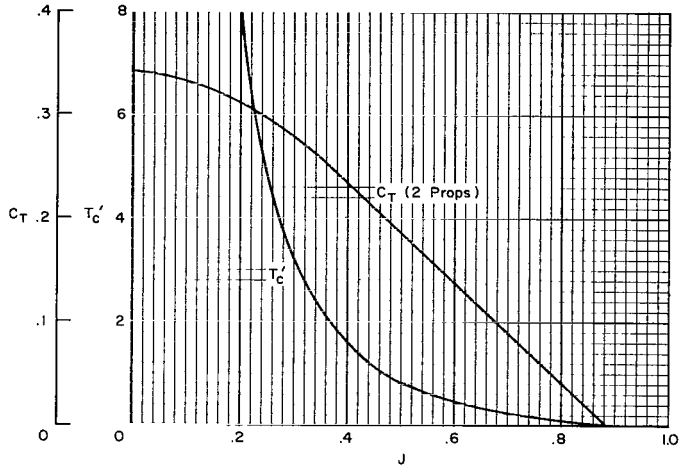

(e) Propeller thrust characteristics.

Figure 2.- Concluded.

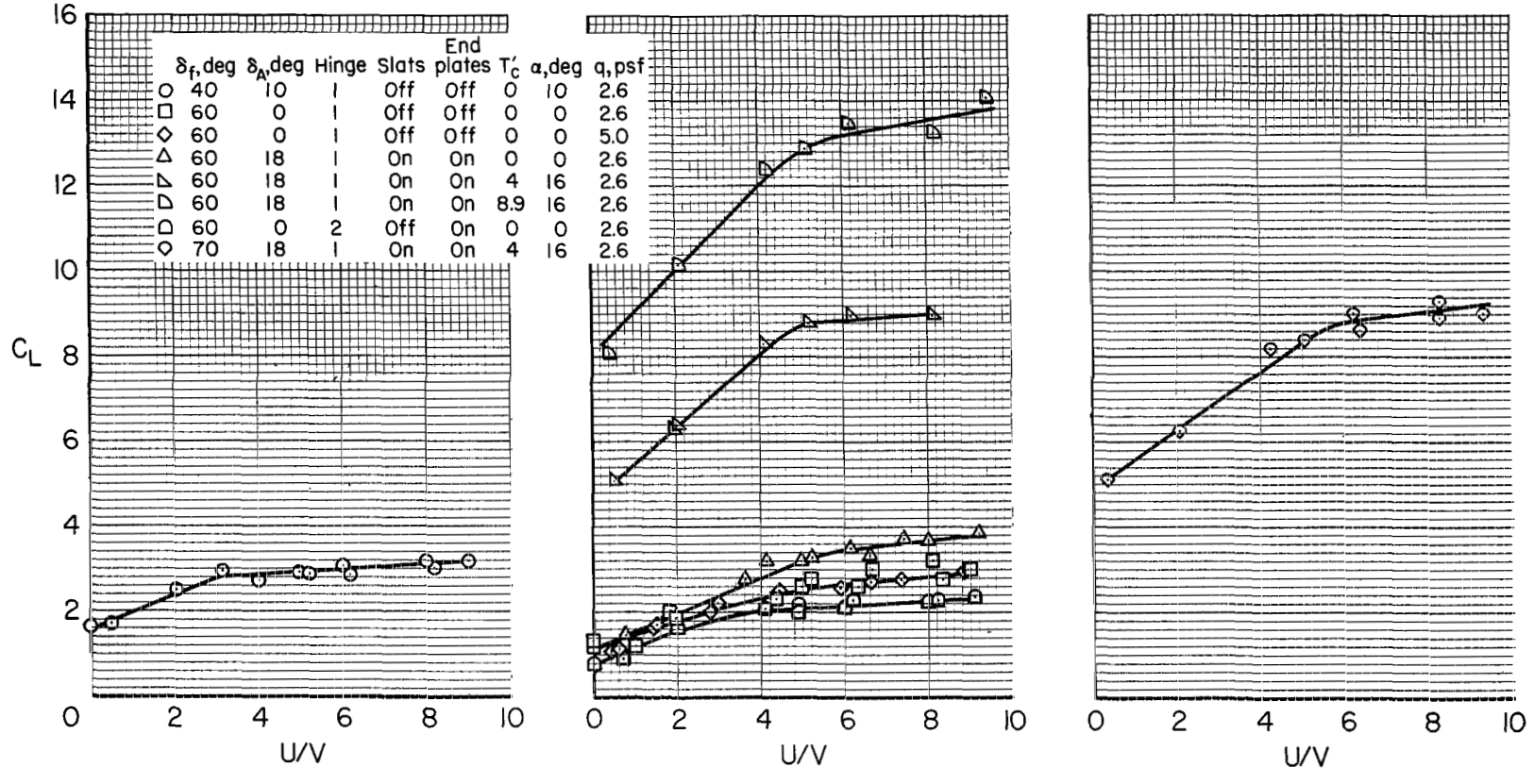

(a) $\delta_f = 40^\circ$, $\delta_A = 10^\circ$ (b) $\delta_f = 60^\circ$ (c) $\delta_f = 70^\circ$, $\delta_A = 18^\circ$

Figure 3.- Effect of cylinder rotation.

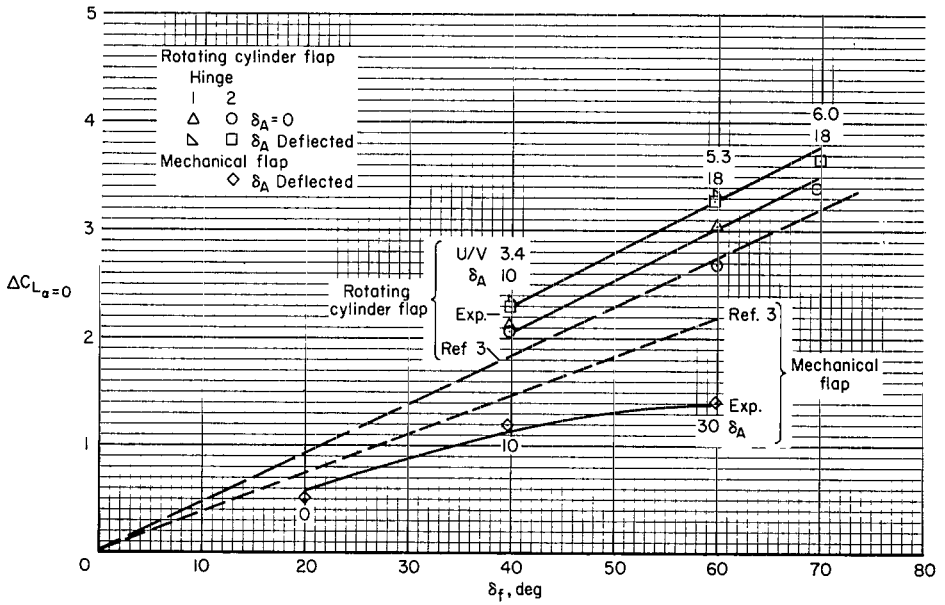

Figure 4.- Flap effectiveness and cylinder speed requirements.

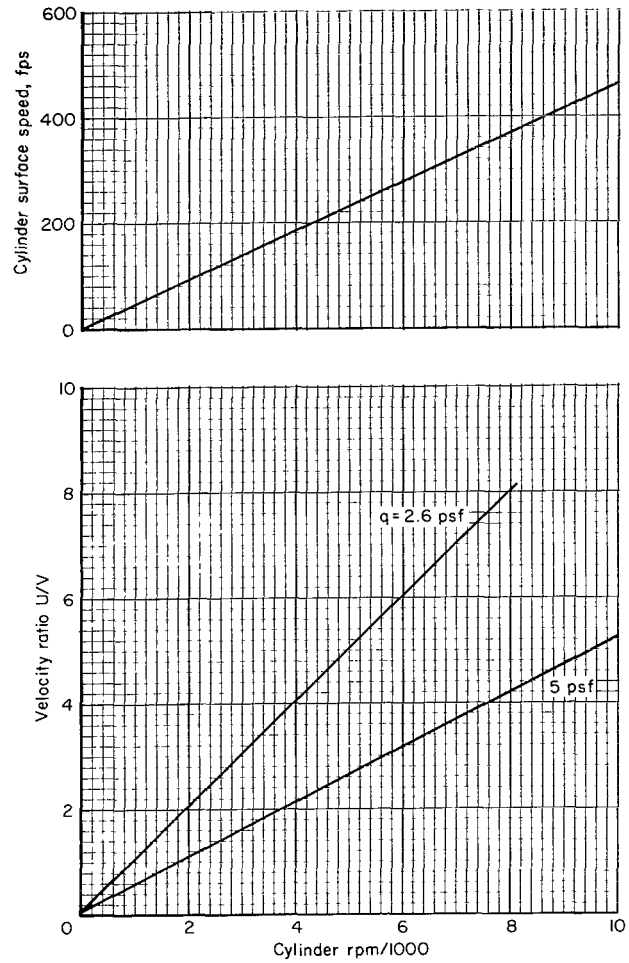

Figure 5.- Cylinder peripheral speed as a function of rpm and dynamic pressure; D = 10.9 in.

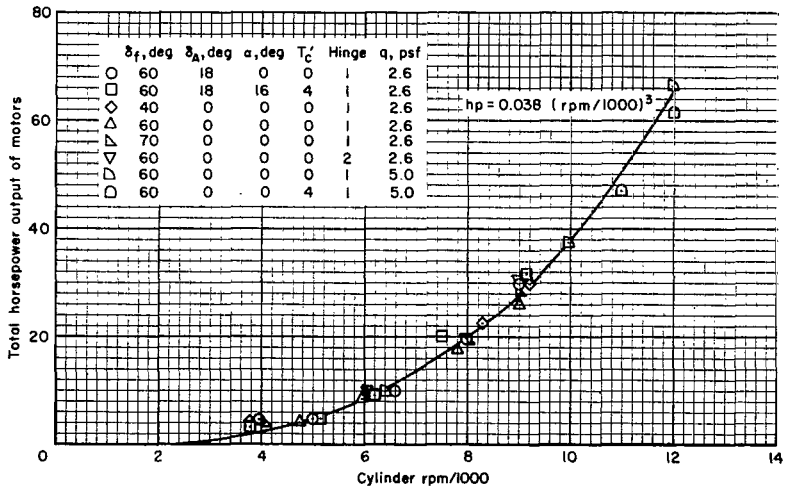

Figure 6.- Cylinder power requirements.

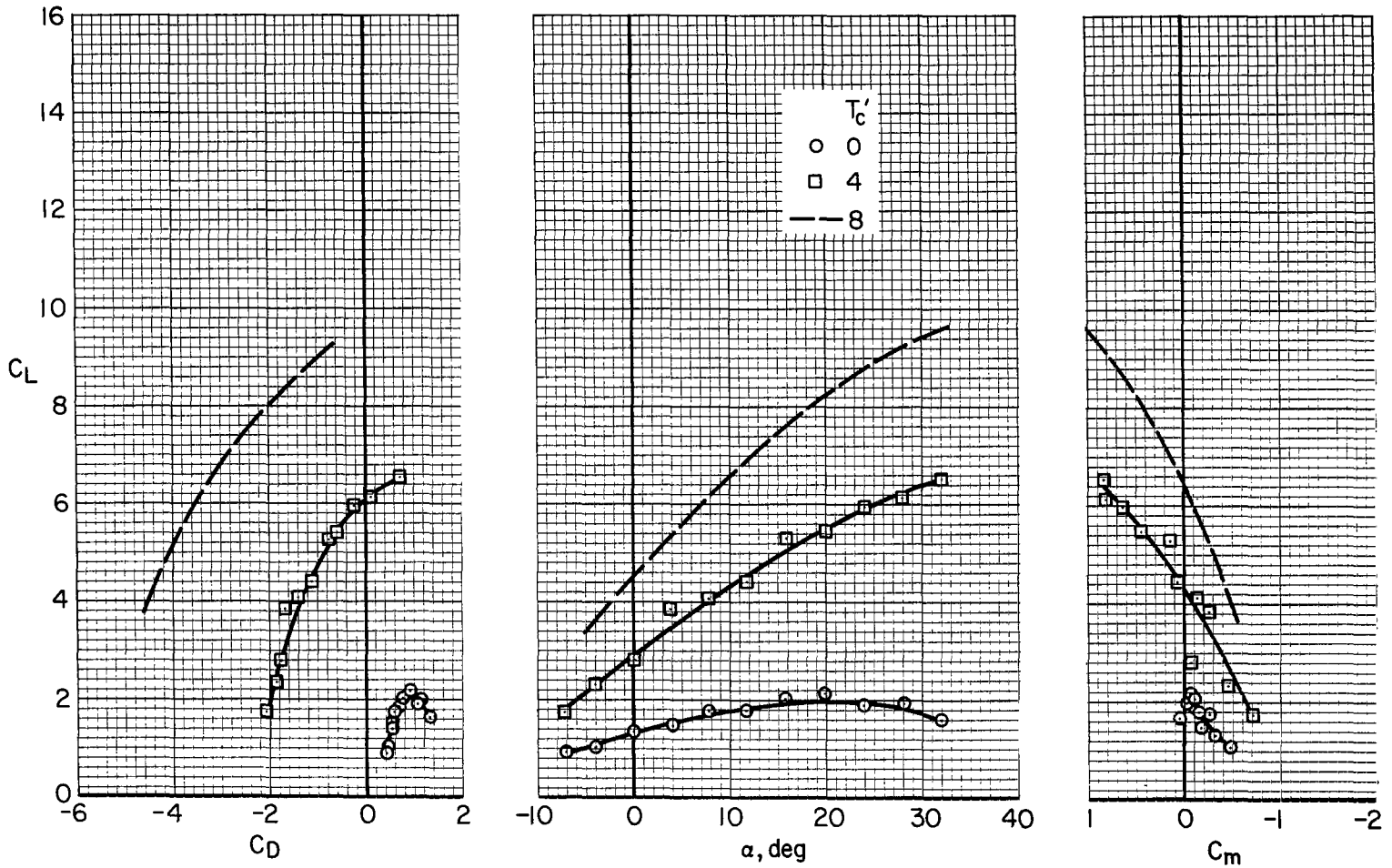

Figure 7.- Aerodynamic characteristics with cylinders stopped, U/V = 0; $\delta_f = 60^\circ$, $\delta_A = 18^\circ$, hinge 1, end plates off.

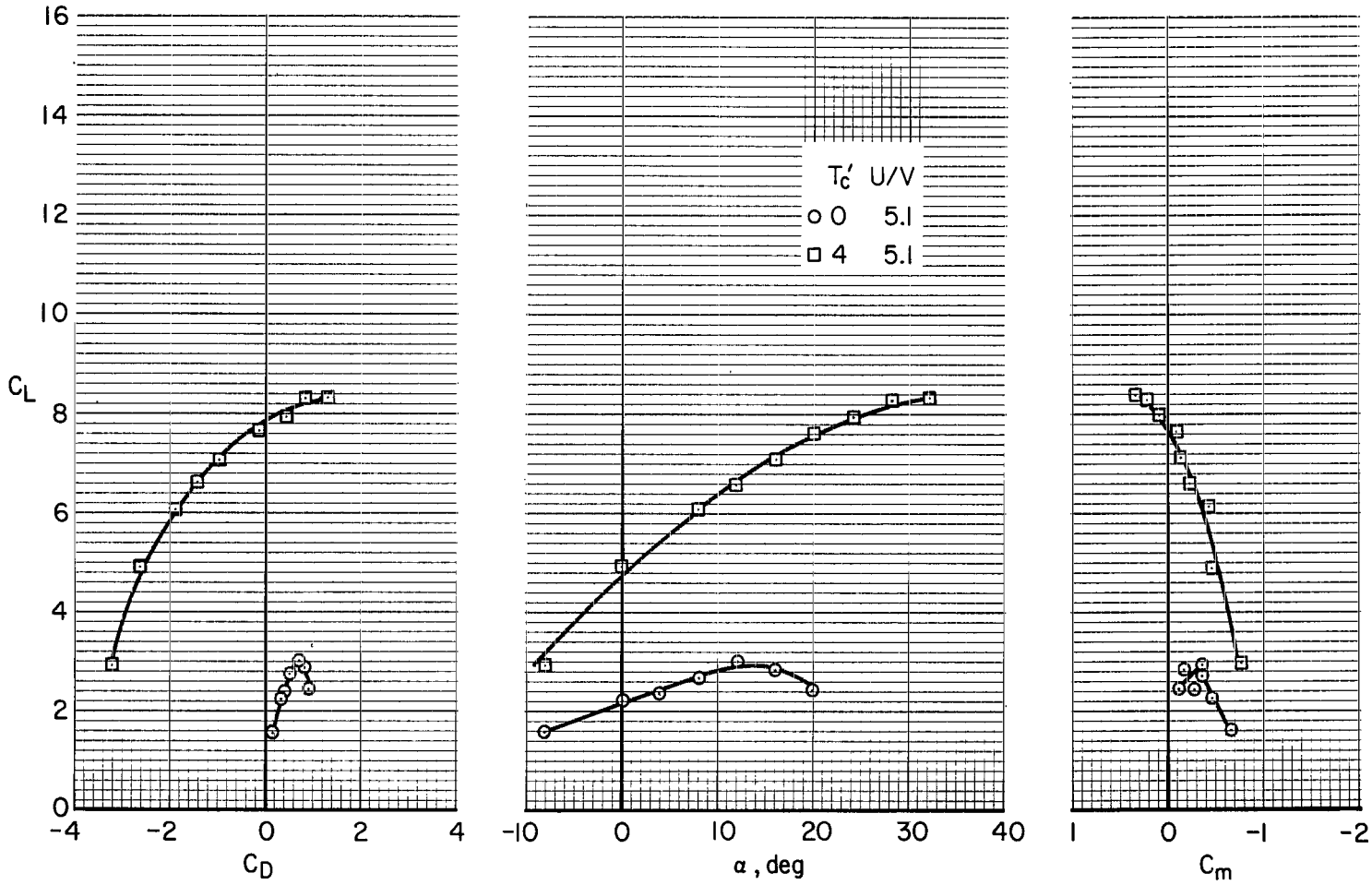

(a) $\delta_f = 40^\circ$, $\delta_A = 0^\circ$

Figure 8.- Longitudinal characteristics, flapevator 0, hinge 1.

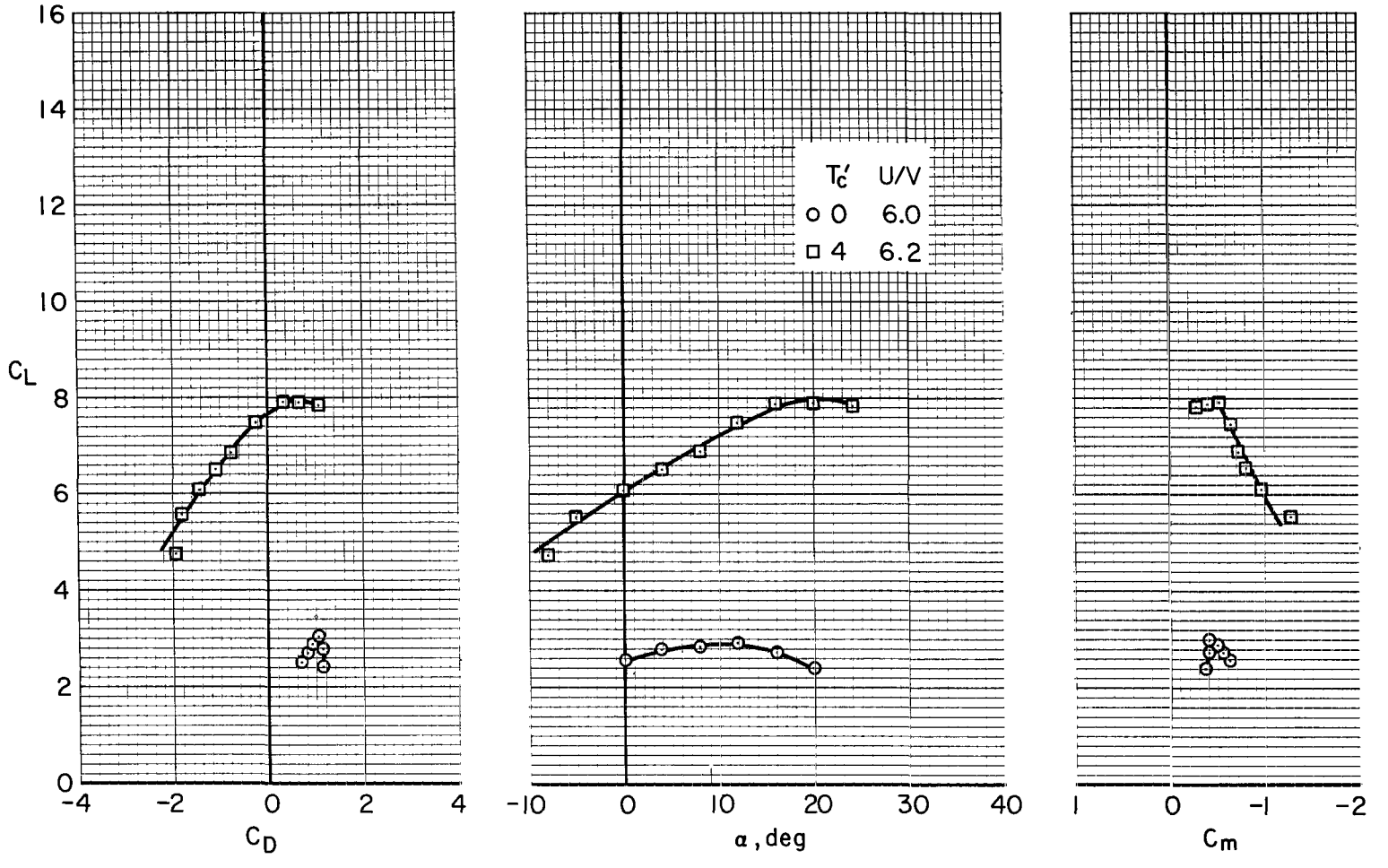

(b) $\delta_f = 60^\circ$, $\delta_A = 0^\circ$

Figure 8.- Continued.

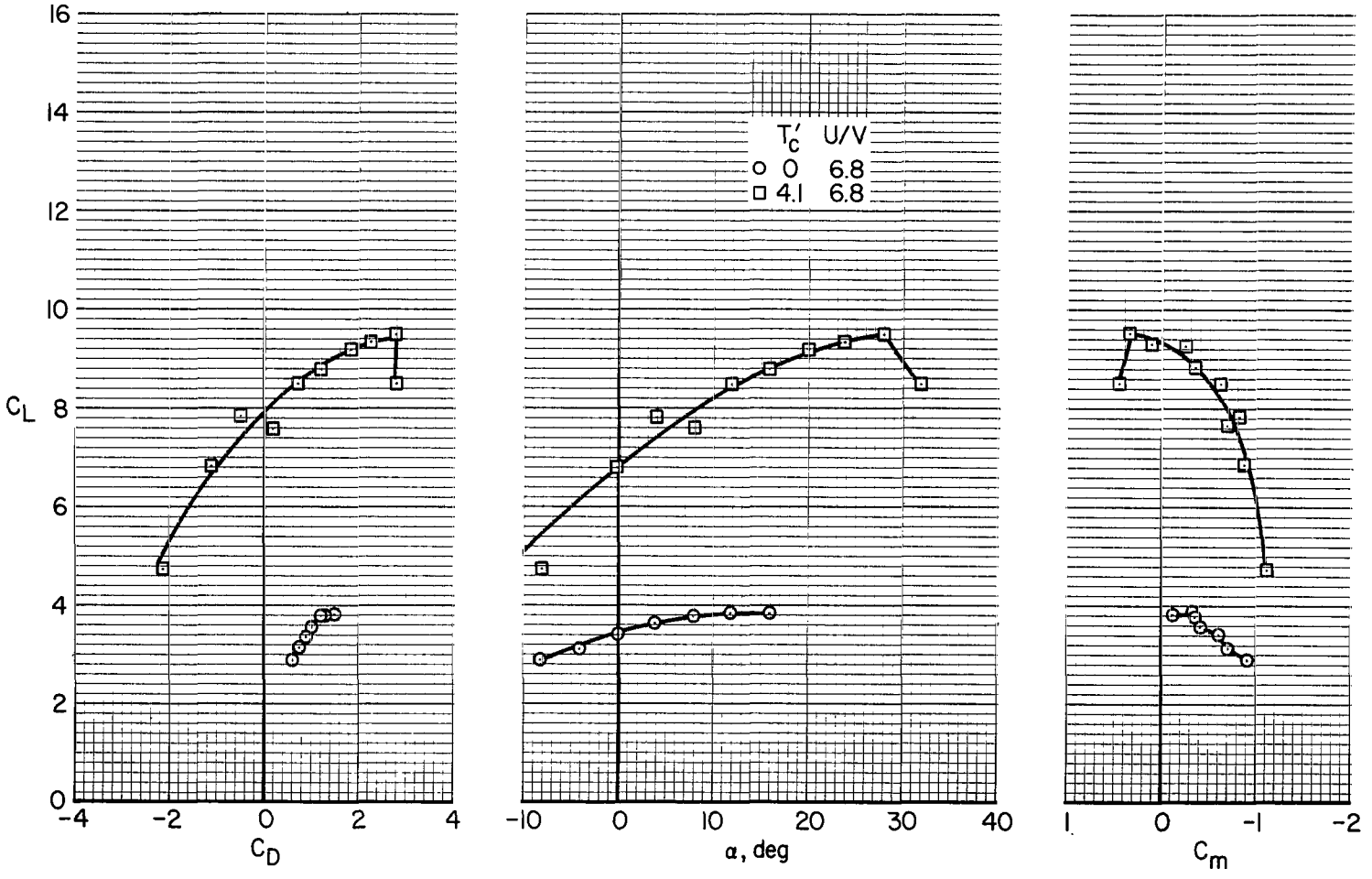

(c) $\delta_f = 70^\circ$, $\delta_A = 0^\circ$, slats on.

Figure 8.- Concluded.

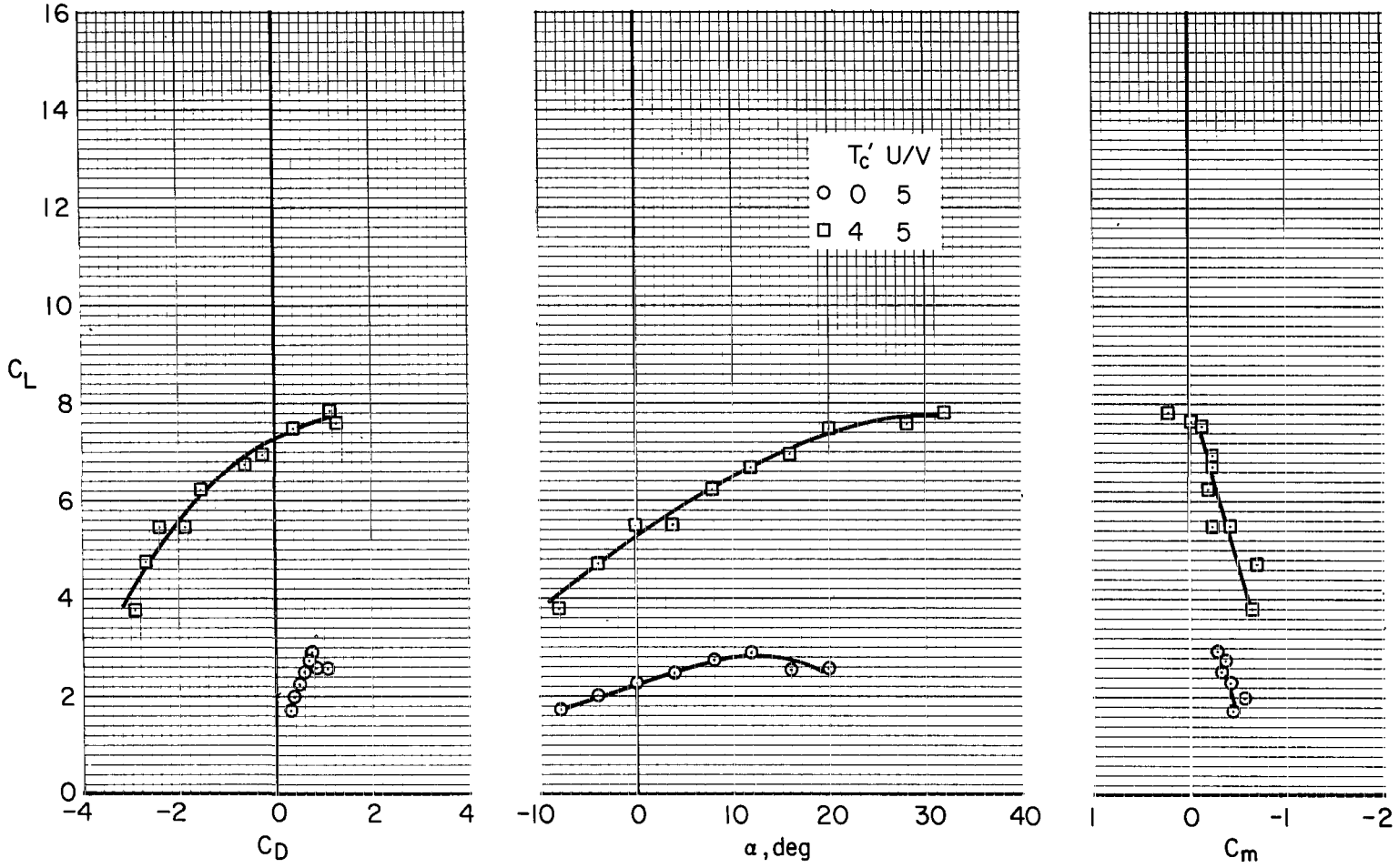

(a) $\delta_f = 40^\circ$, $\delta_A = 10^\circ$

Figure 9.- Longitudinal characteristics, flapevator deflected, hinge 1.

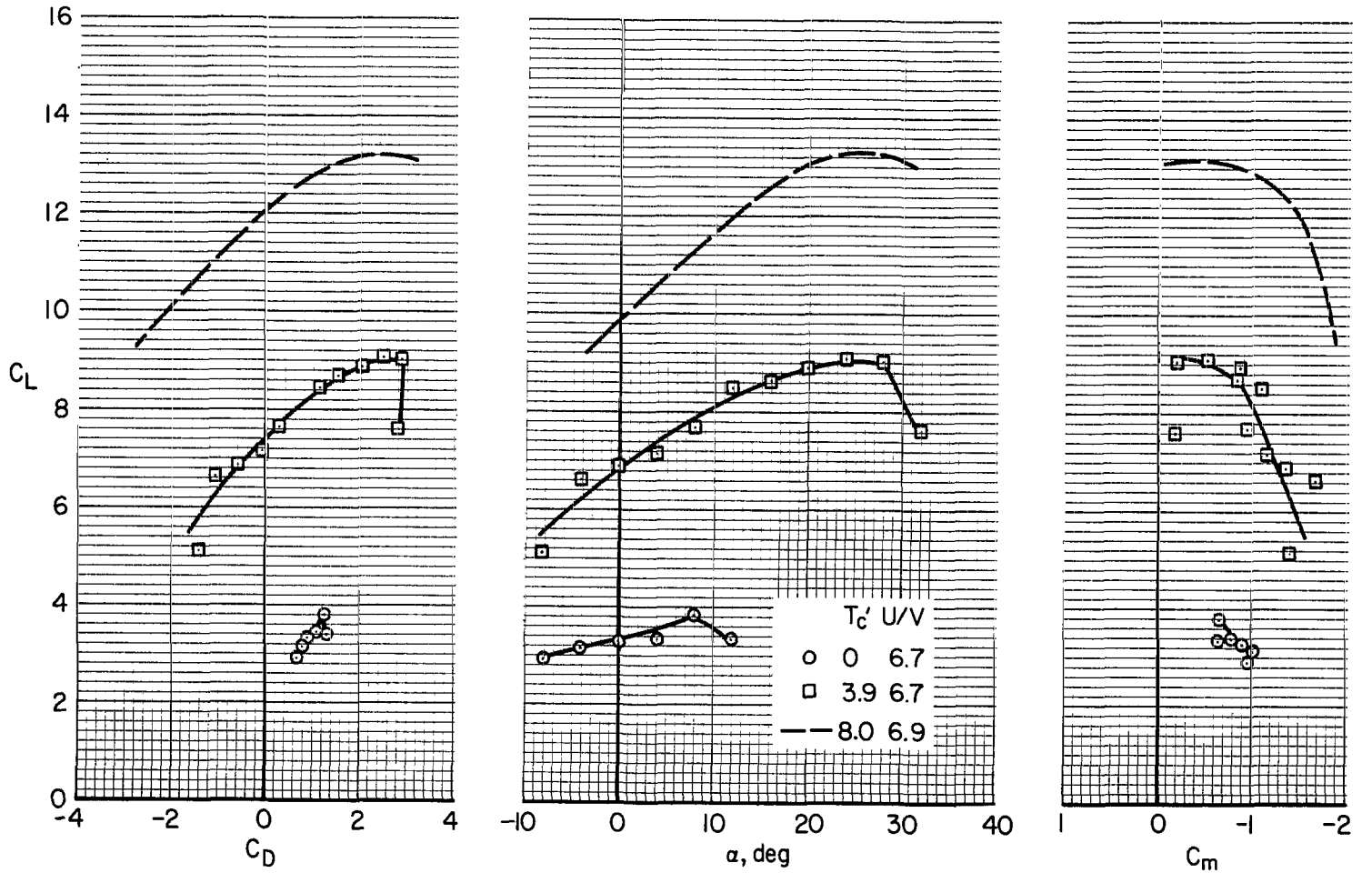

(b) $\delta_f = 60^\circ$, $\delta_A = 18^\circ$

Figure 9.- Continued.

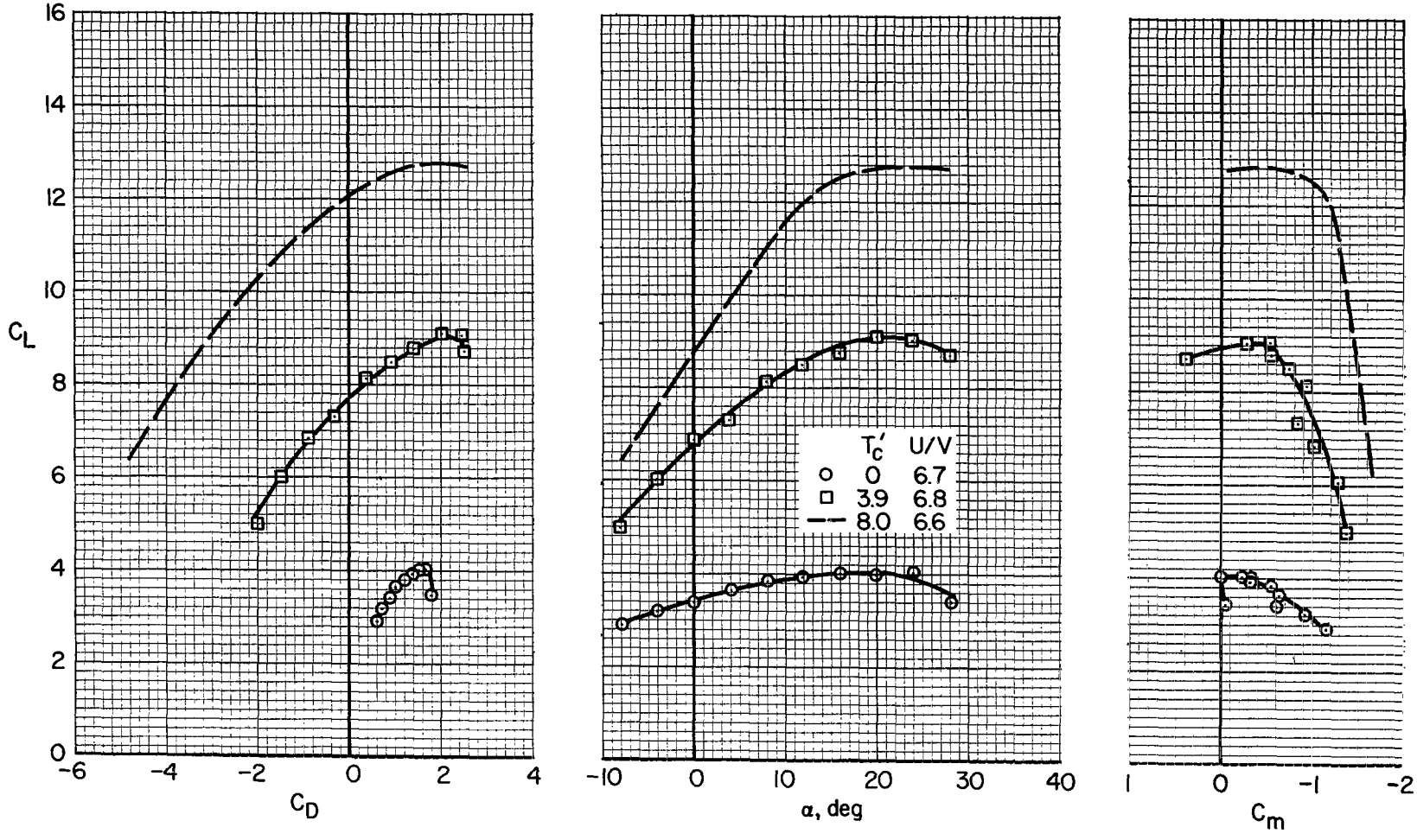

(c) $\delta_f = 60^\circ$, $\delta_A = 18^\circ$, slats on.

Figure 9.- Continued.

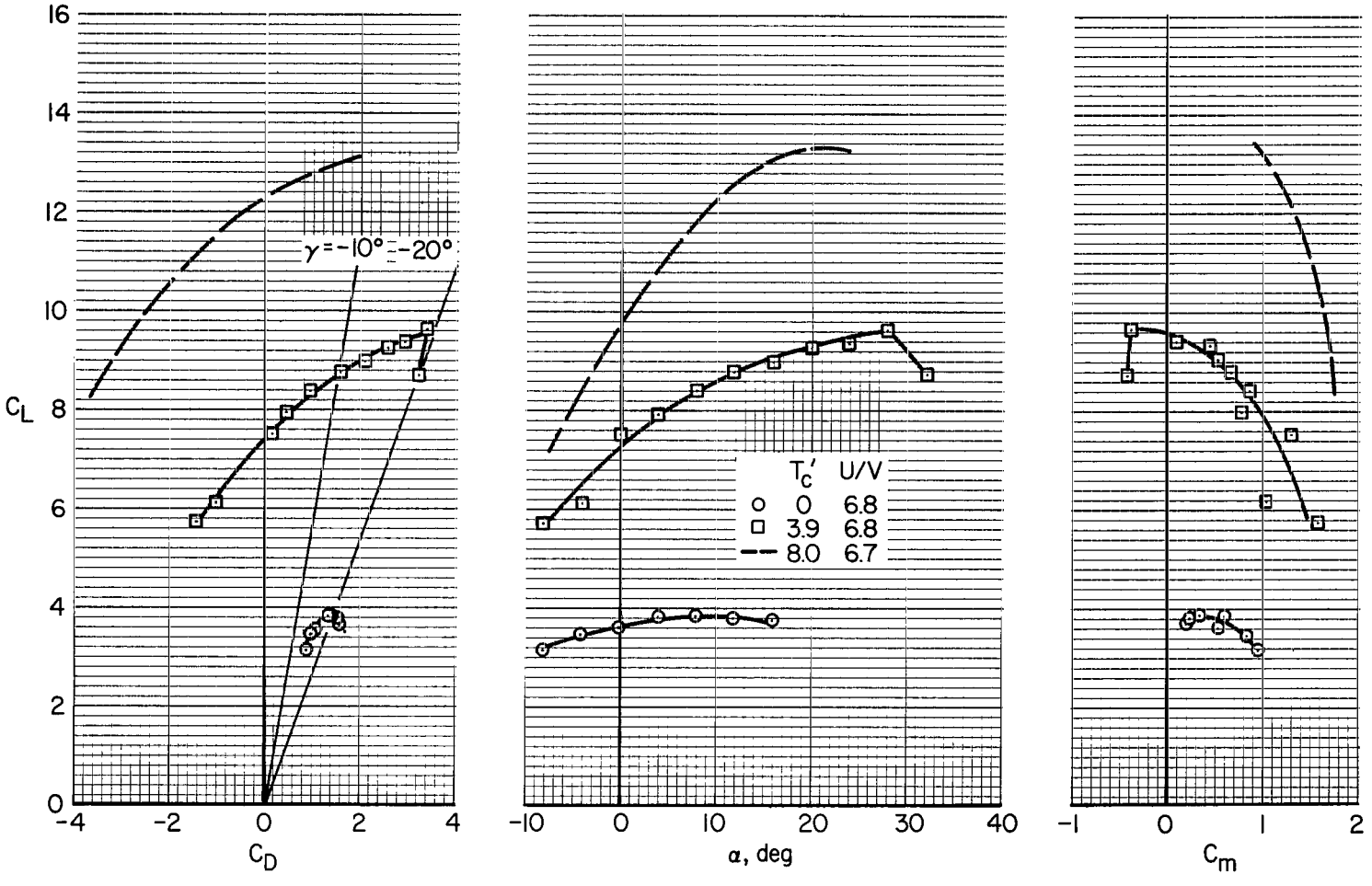

(d) $\delta_f = 70^\circ$, $\delta_A = 18^\circ$, slats on.

Figure 9.- Concluded.

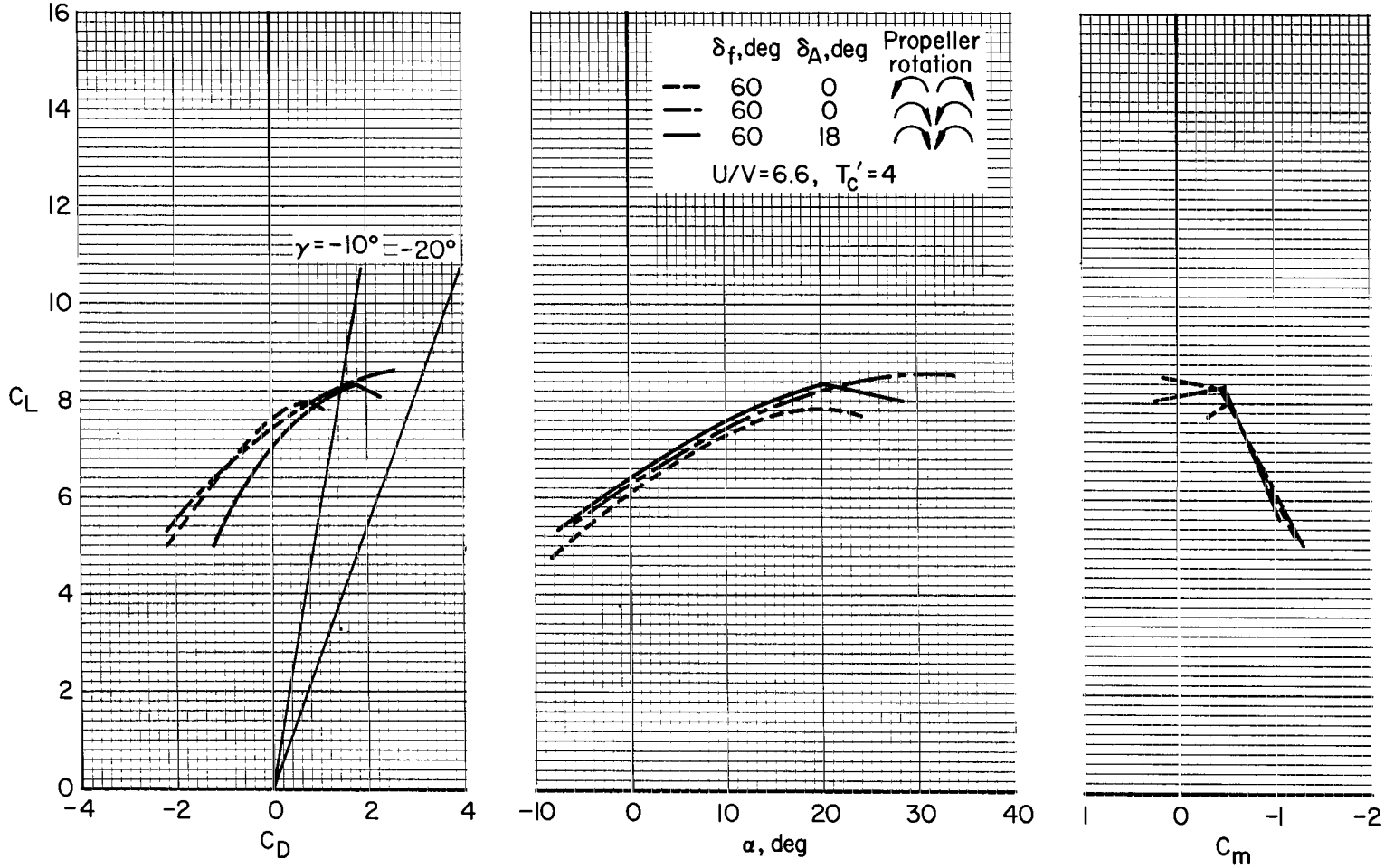

(a) Effect of propeller rotation and flapevator deflection; slats off, end plates off.

Figure 10.- Effect of various devices on the longitudinal characteristics, hinge 1.

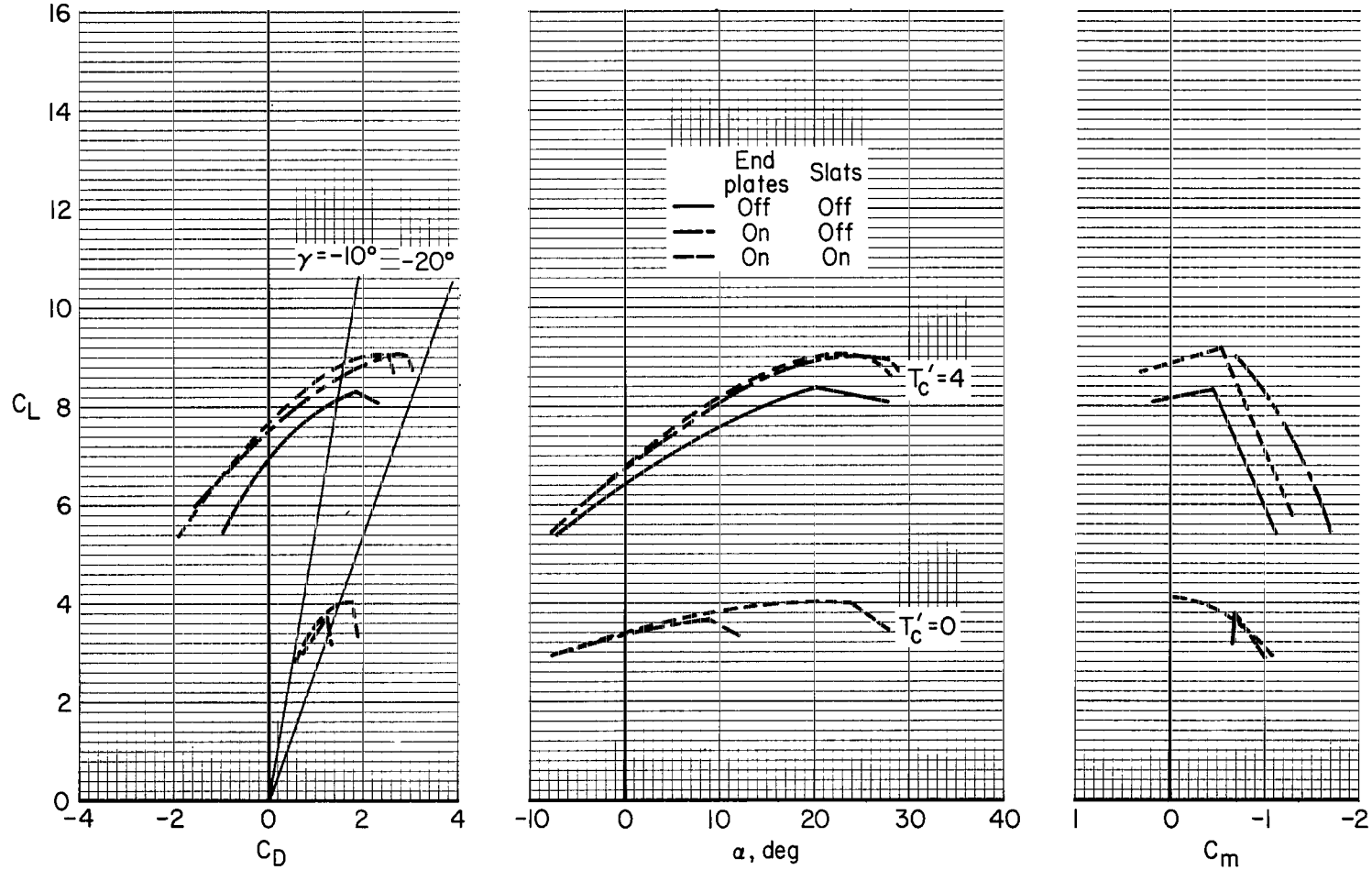

(b) Effect of end plates and slats; $\delta_f = 60^\circ$, $\delta_A = 18^\circ$, U/V = 6.6.

Figure 10.- Concluded.

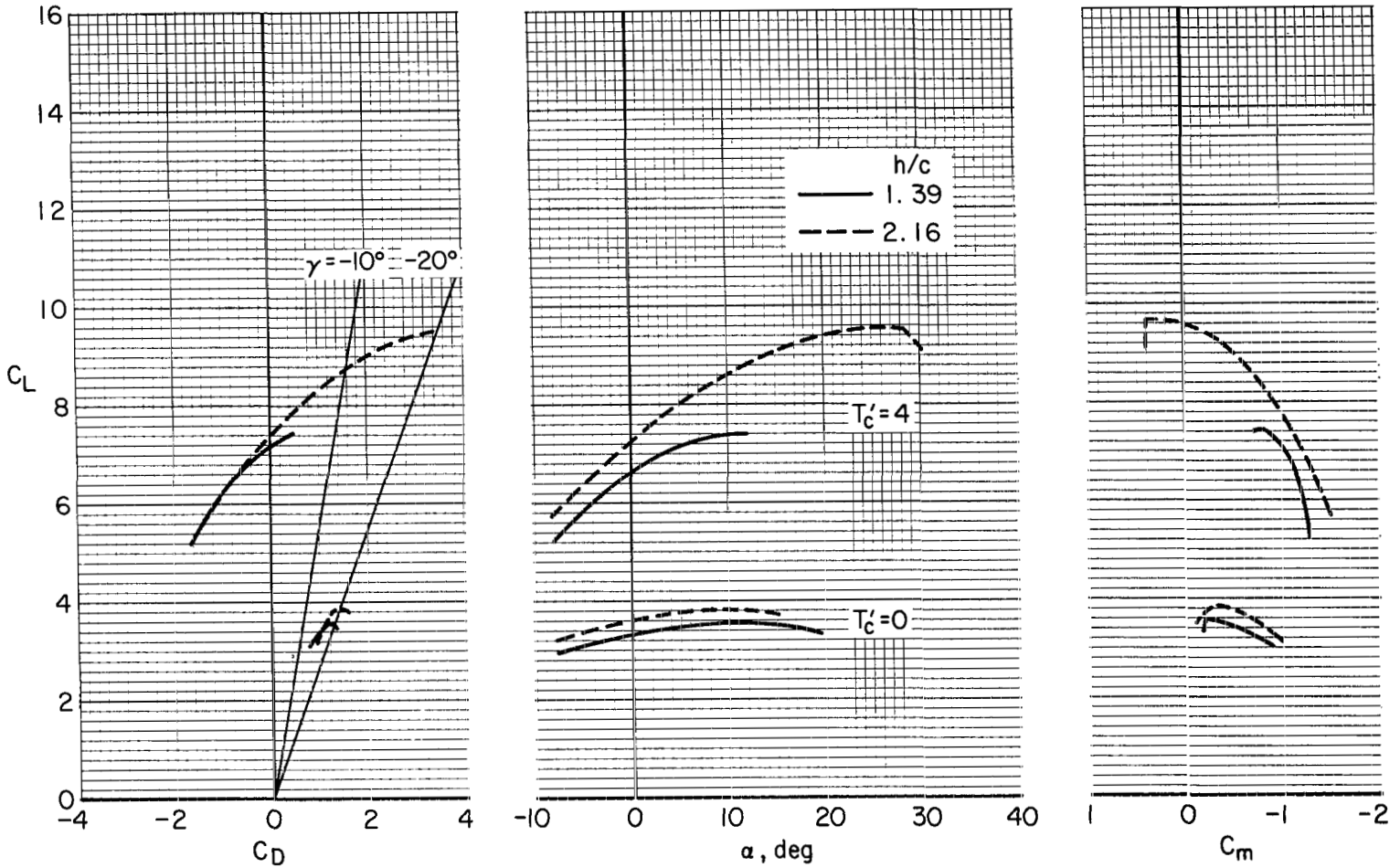

Figure 11.- Effect of ground height on the aerodynamic characteristics; $\delta_f = 70°$, $\delta_A = 18°$, slats and end plates on, hinge 1.

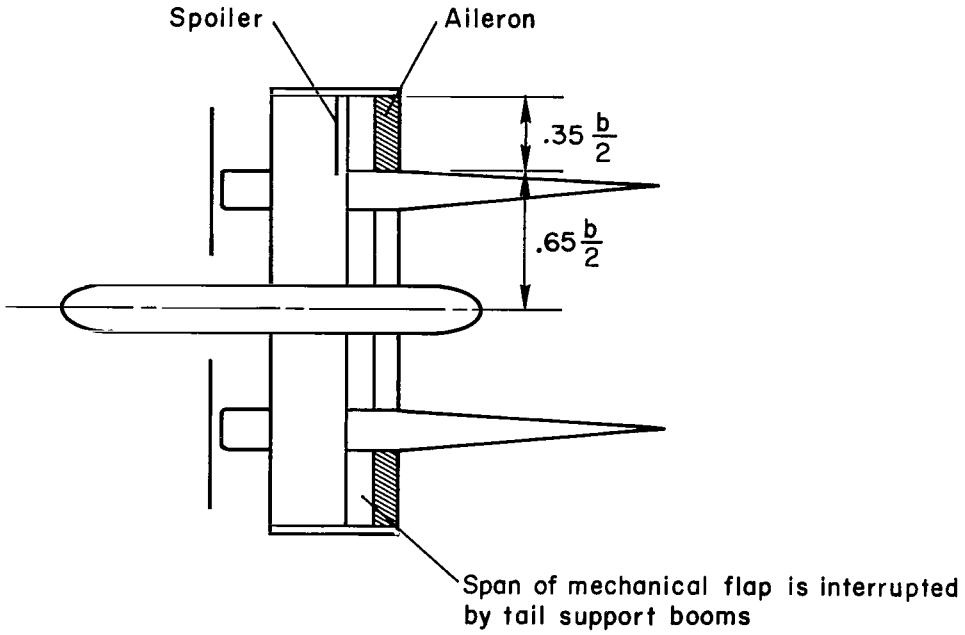

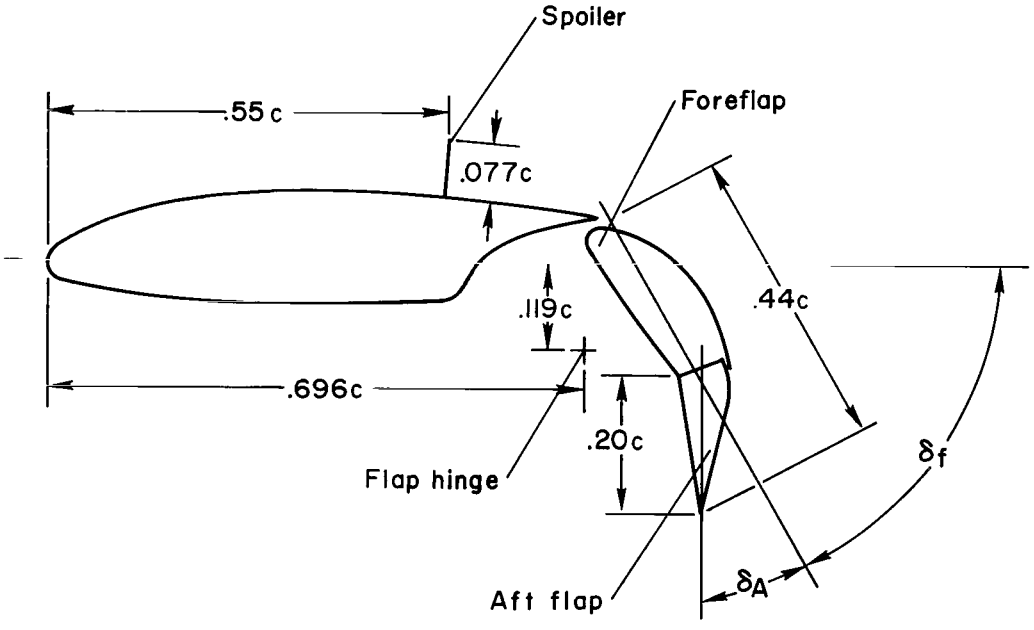

Figure 12.- Mechanical flap geometry.

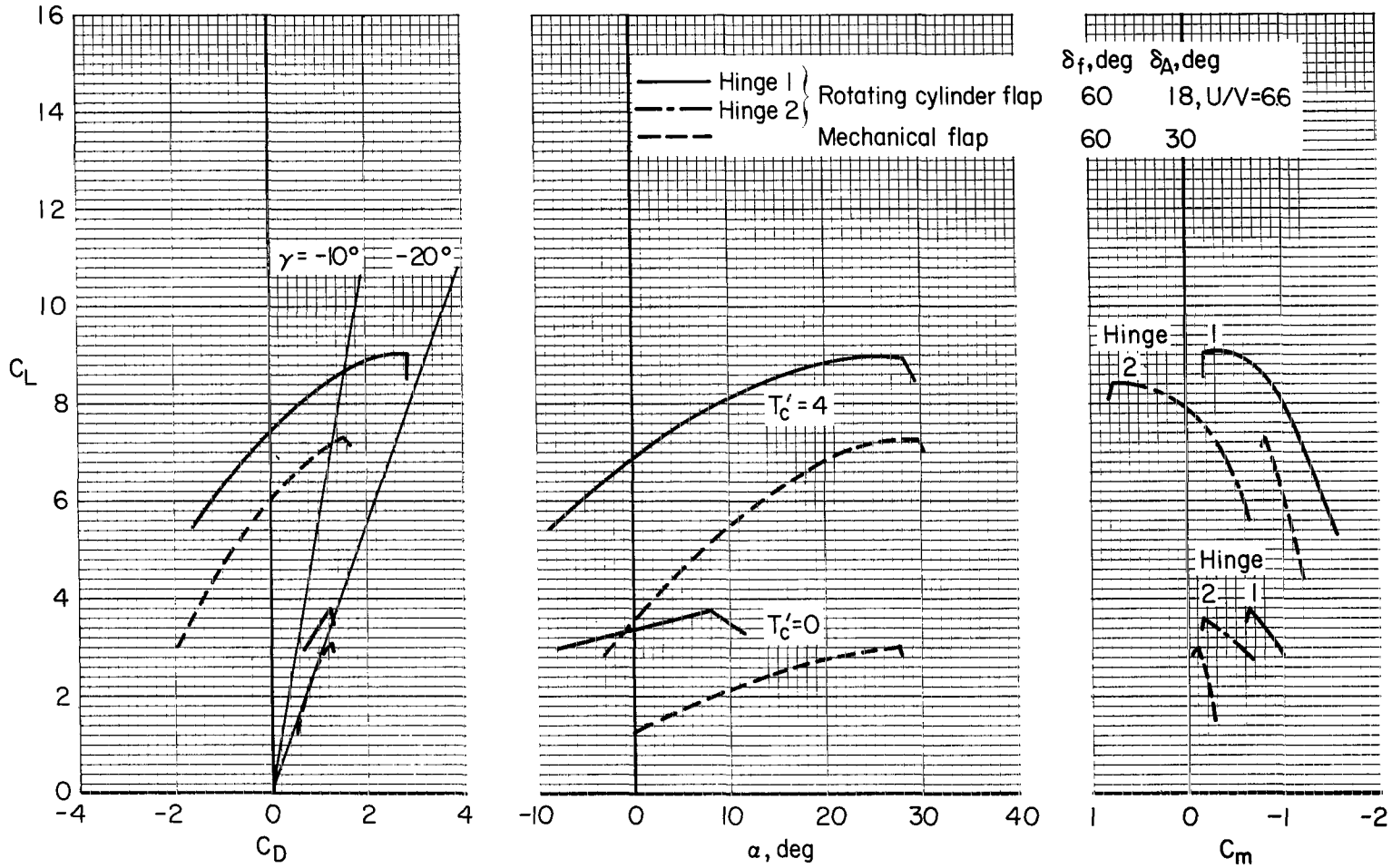

(a) Longitudinal characteristics.

Figure 13.- Comparison with mechanical flap; slats on, tail off.

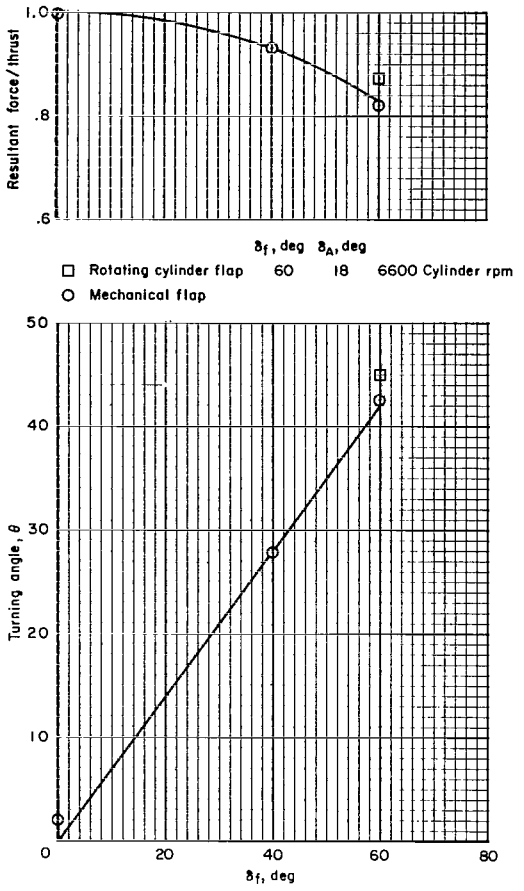

(b) Static hover characteristics.

Figure 13.- Concluded.

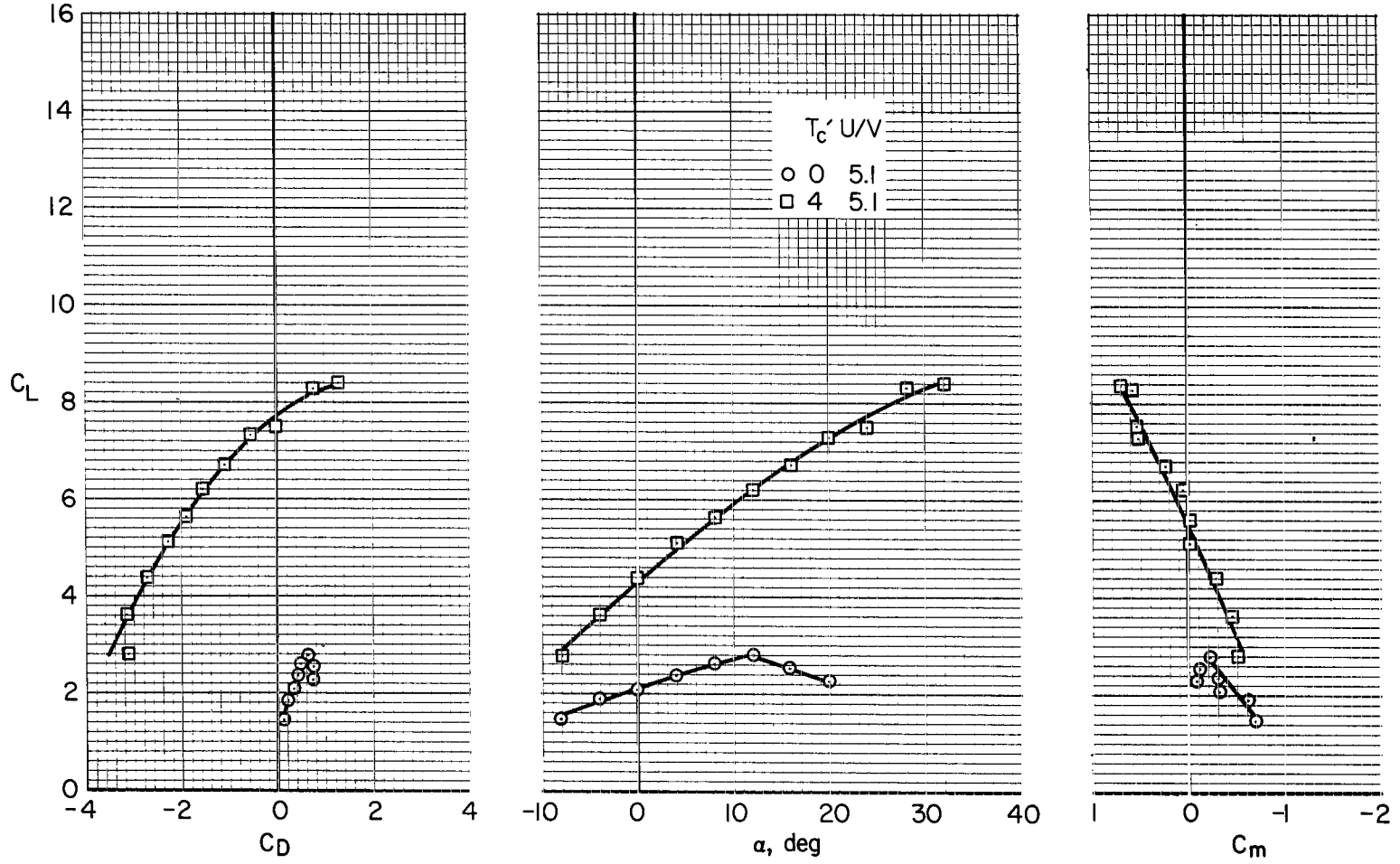

(a) $\delta_f = 40^\circ$, $\delta_A = 0^\circ$

Figure 14.- Longitudinal characteristics, flapevator 0, hinge 2.

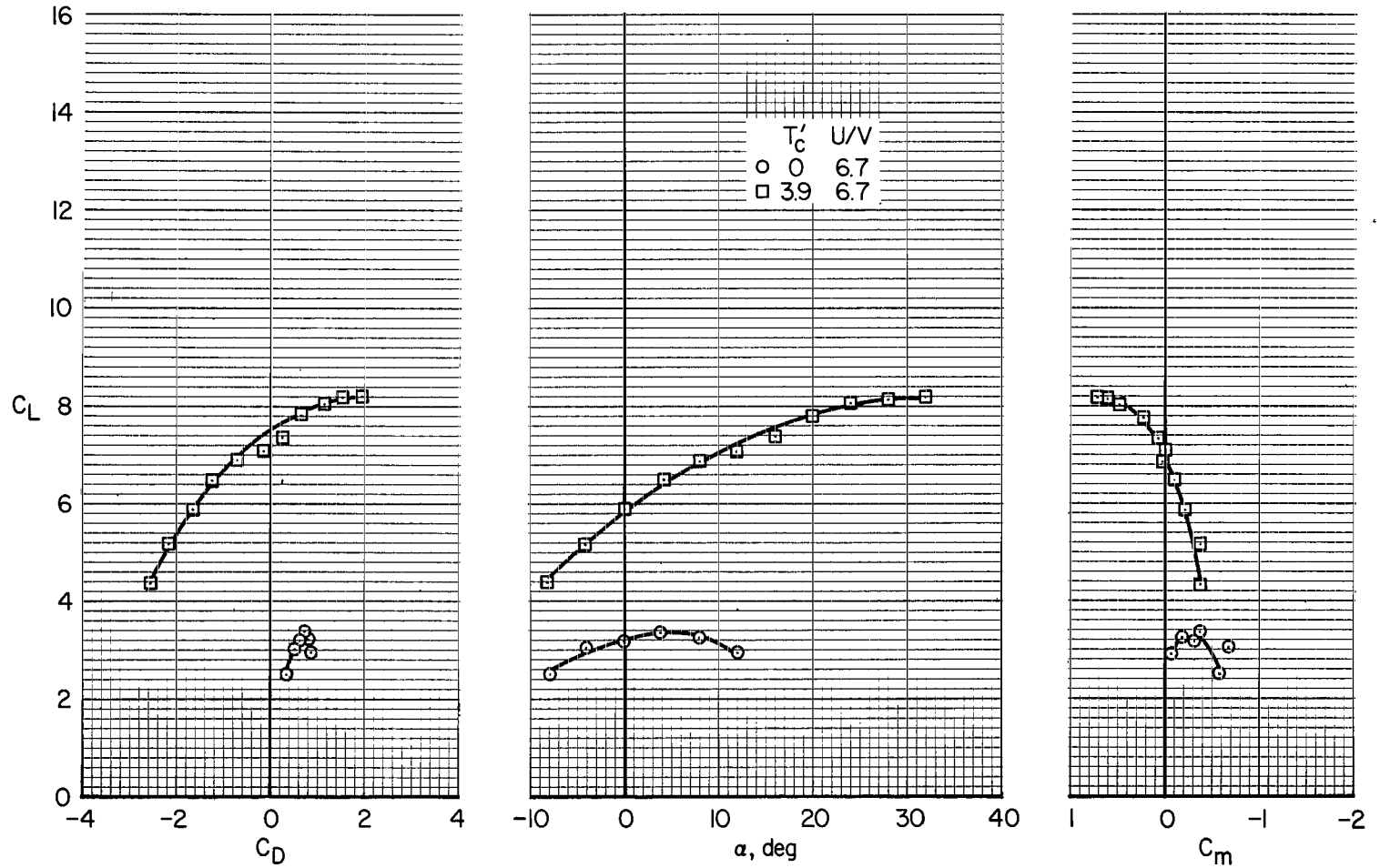

(b) $\delta_f = 60^\circ$, $\delta_A = 0^\circ$

Figure 14.- Concluded.

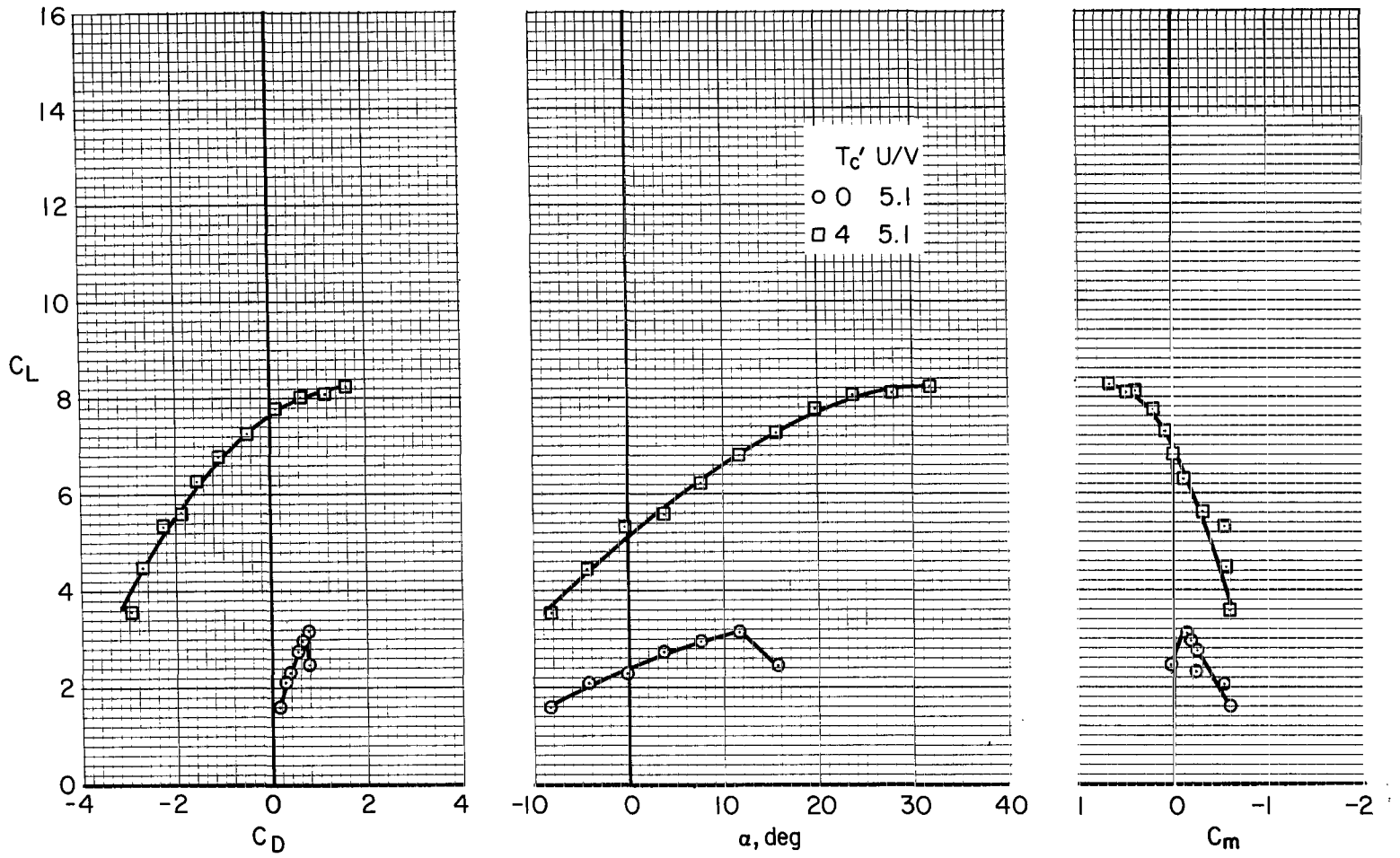

(a) $\delta_f = 40^\circ$, $\delta_A = 10^\circ$

Figure 15.- Longitudinal characteristics, flapevator deflected, hinge 2.

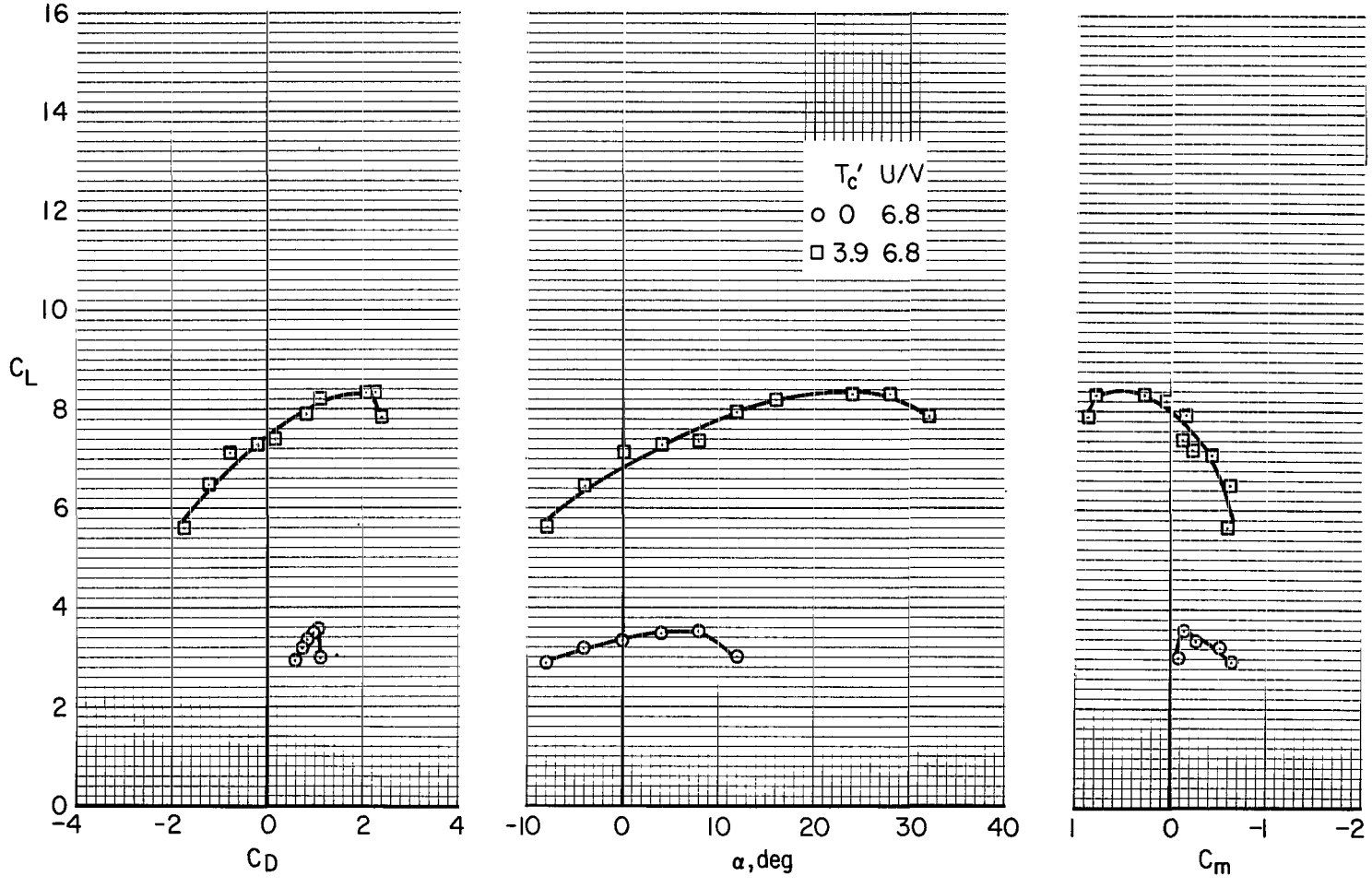

(b) $\delta_f = 60^\circ$, $\delta_A = 18^\circ$

Figure 15.- Concluded.

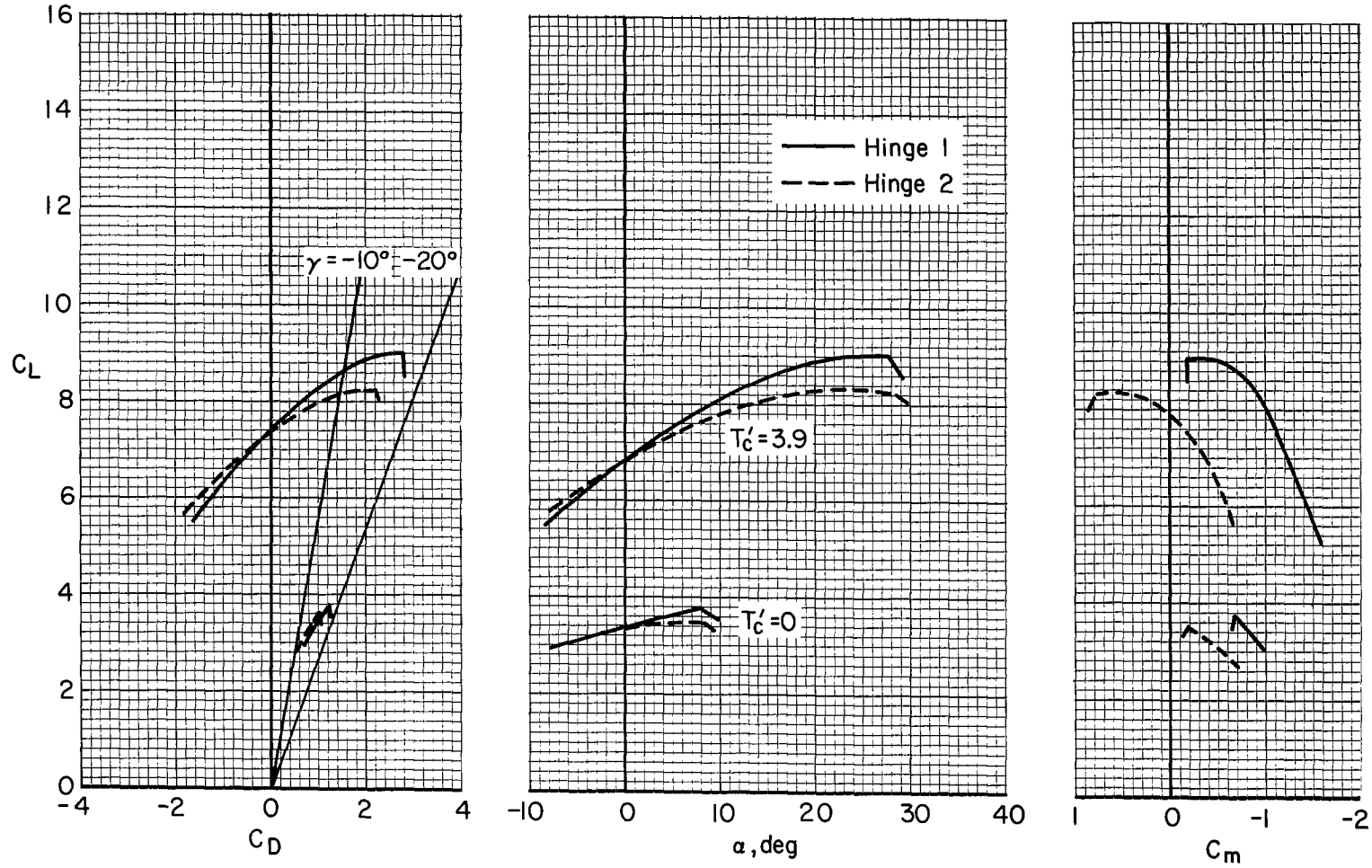

(a) Without flap chord extension.

Figure 16.- Effect of hinge location on aerodynamic characteristics; $\delta_f = 60°$, $\delta_A = 18°$, $U/V = 6.7$.

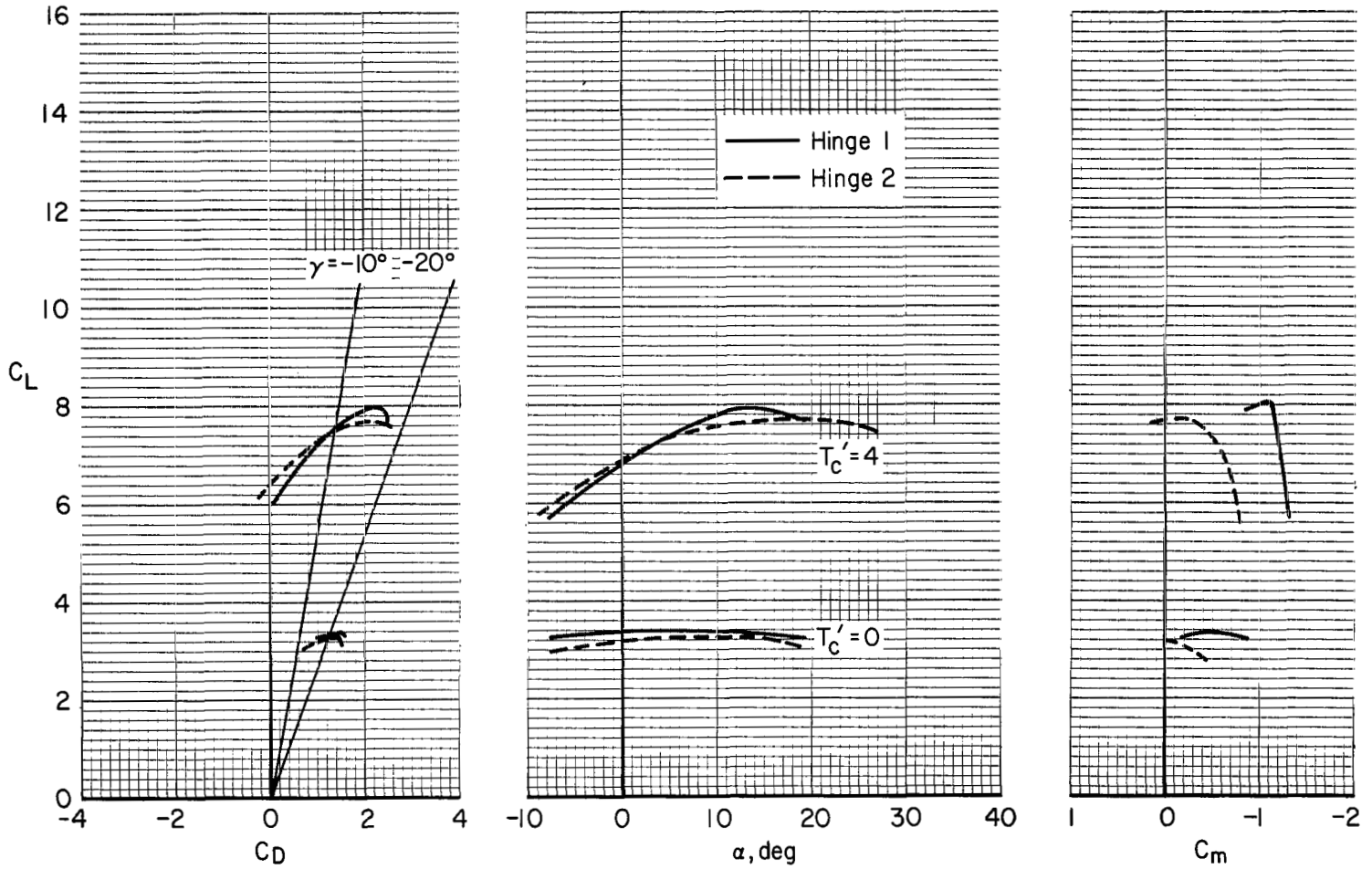

(b) With flap chord extension, slats on.

Figure 16.- Concluded.

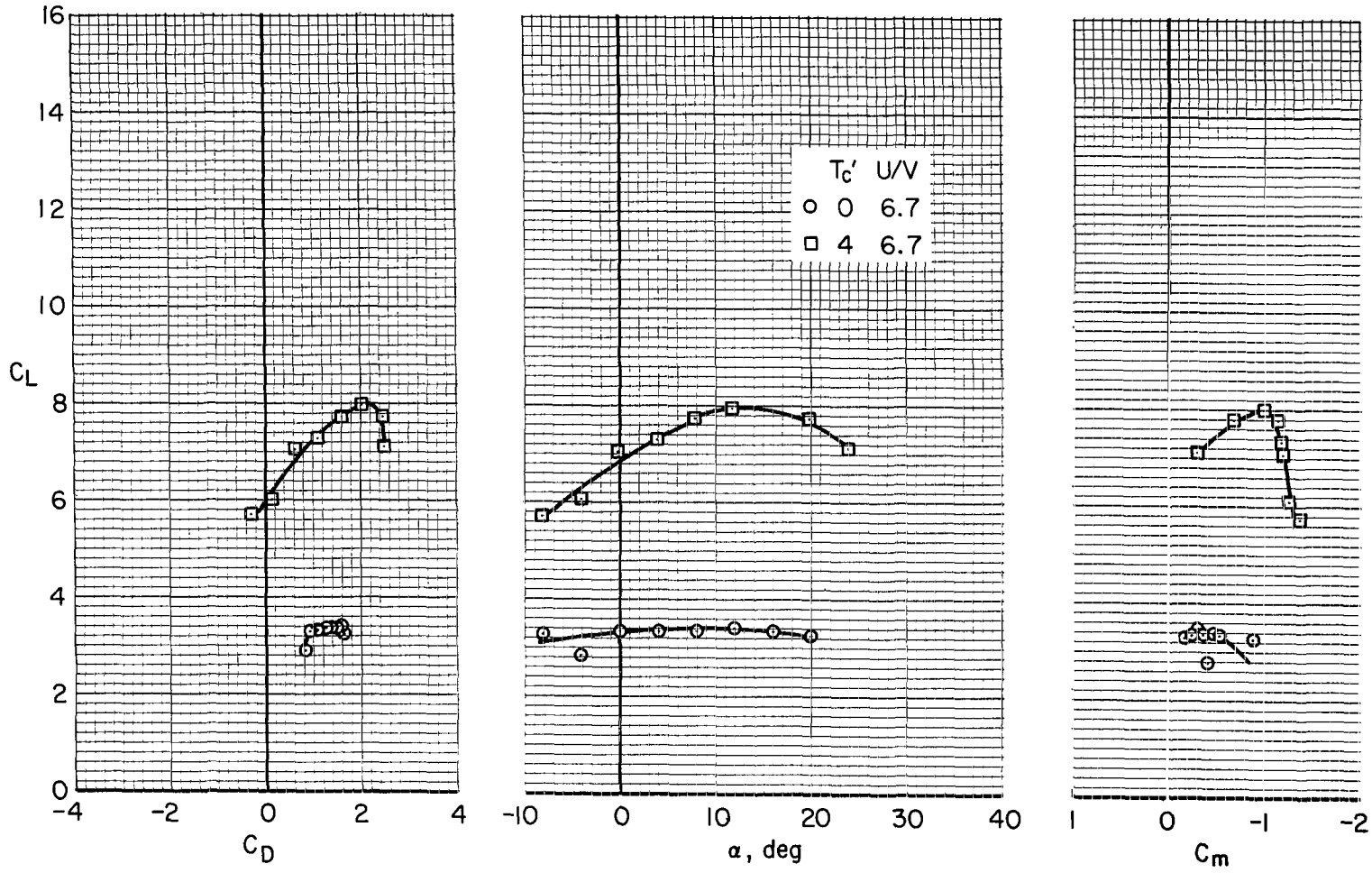

(a) $\delta_f = 60^\circ$, $\delta_A = 18^\circ$, slats on, hinge 1.

Figure 17.- Aerodynamic characteristics with flap chord extension.

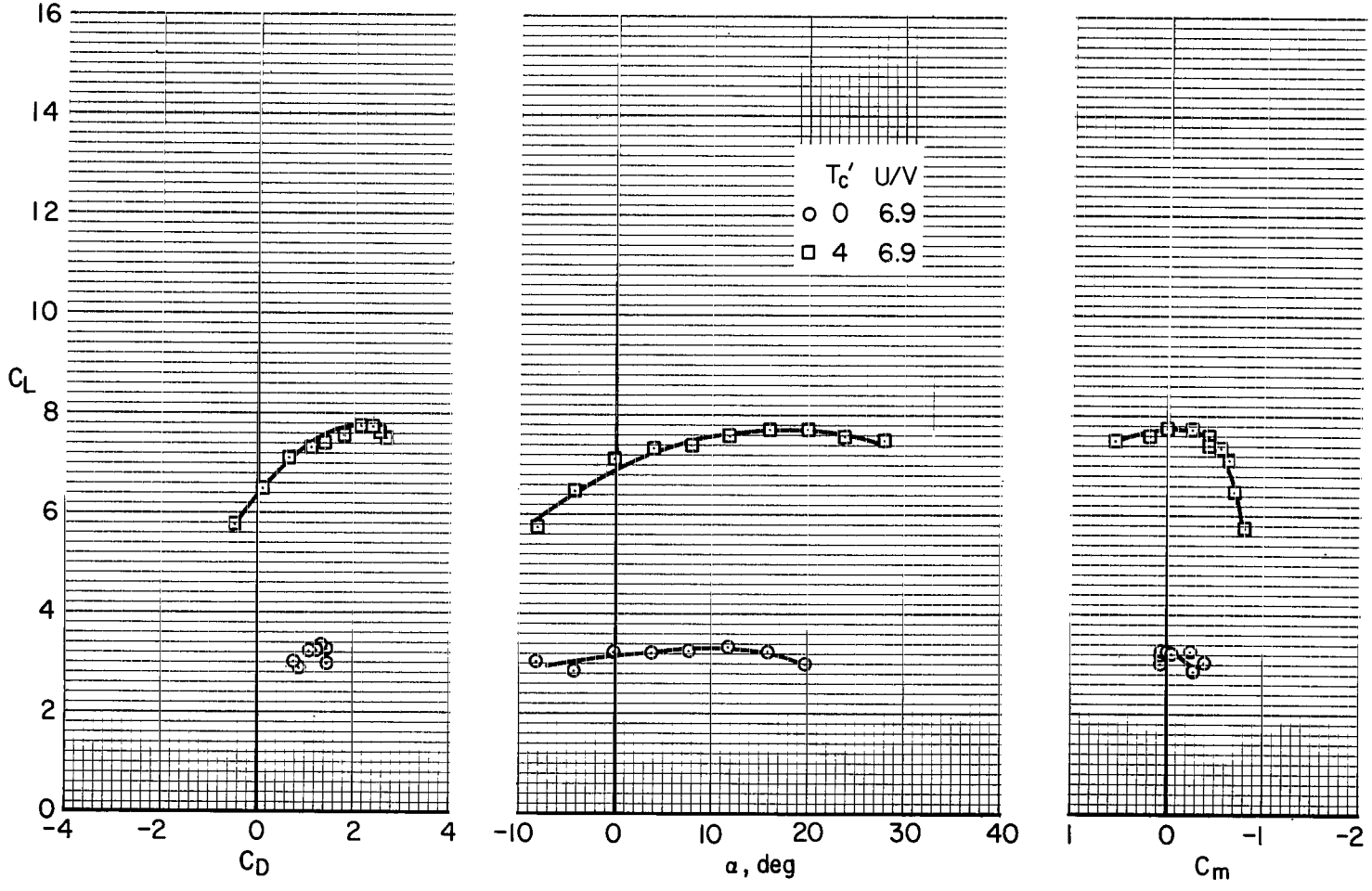

(b) $\delta_f = 60^\circ$, $\delta_A = 18^\circ$, slats on, hinge 2.

Figure 17.- Continued.

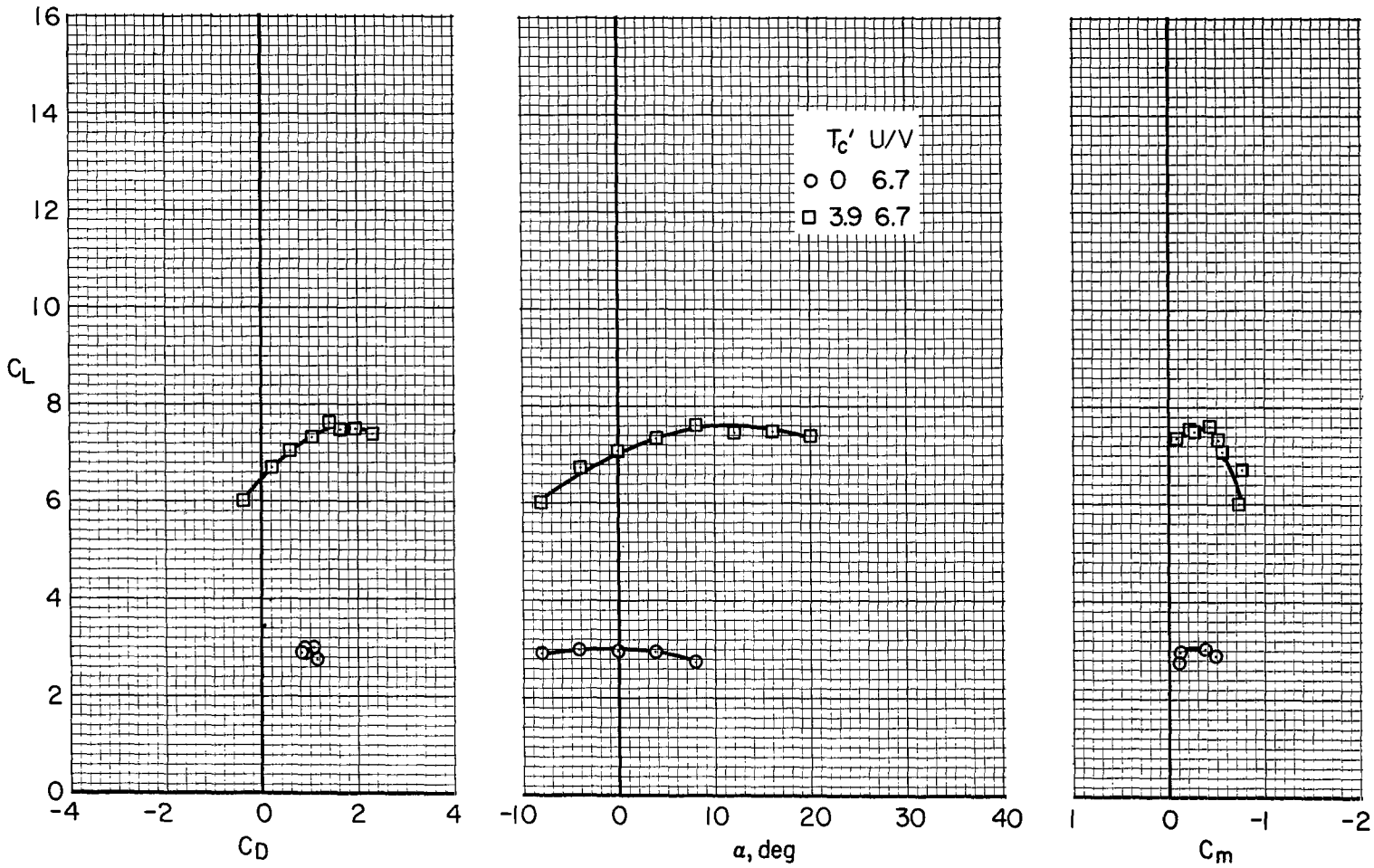

(c) $\delta_f = 60^\circ$, $\delta_A = 18^\circ$, hinge 2.

Figure 17.- Concluded.

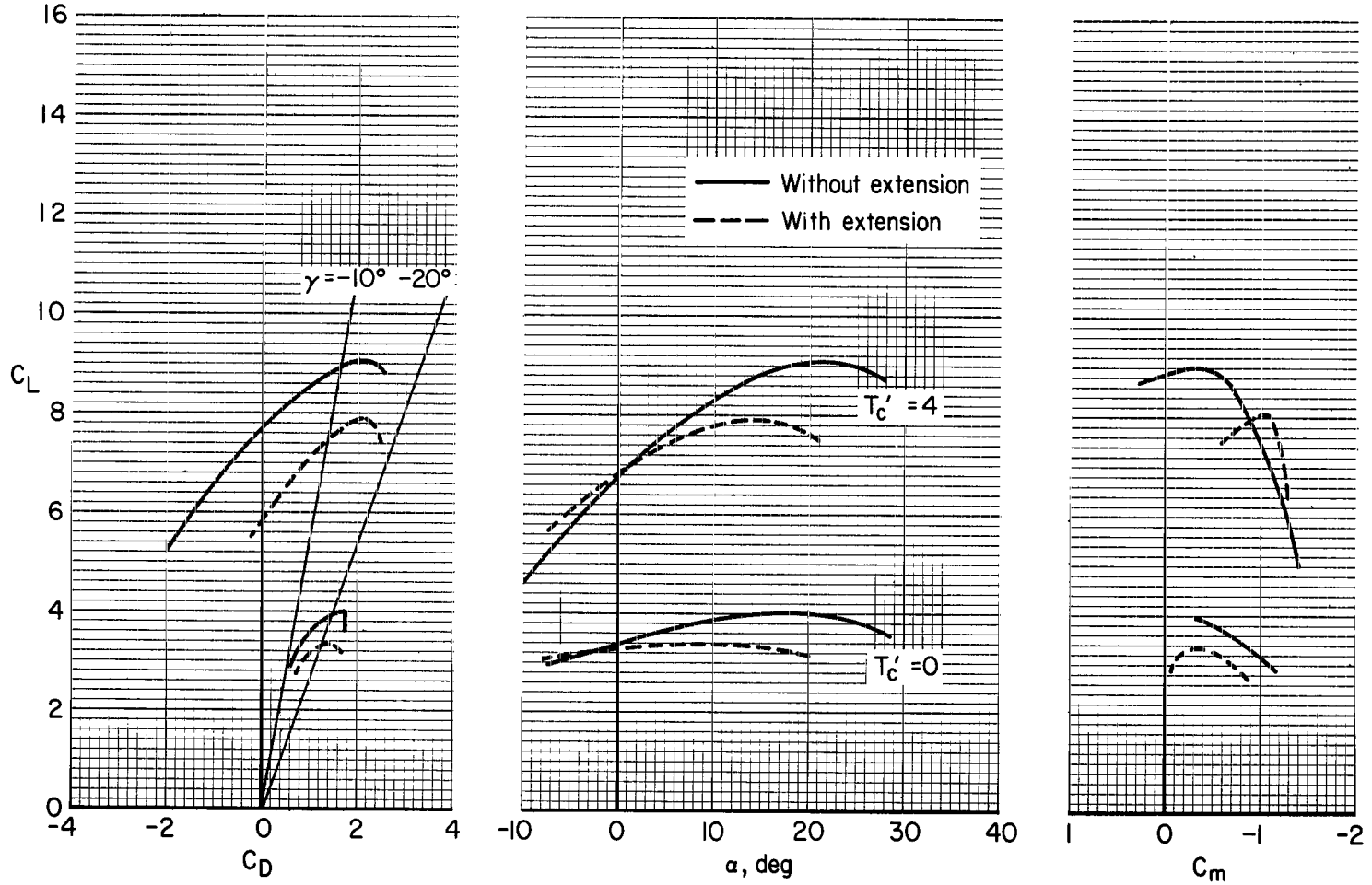

(a) Hinge 1, slats on.

Figure 18.- Effect of flap chord extension; $\delta_f = 60^\circ$, $\delta_A = 18^\circ$.

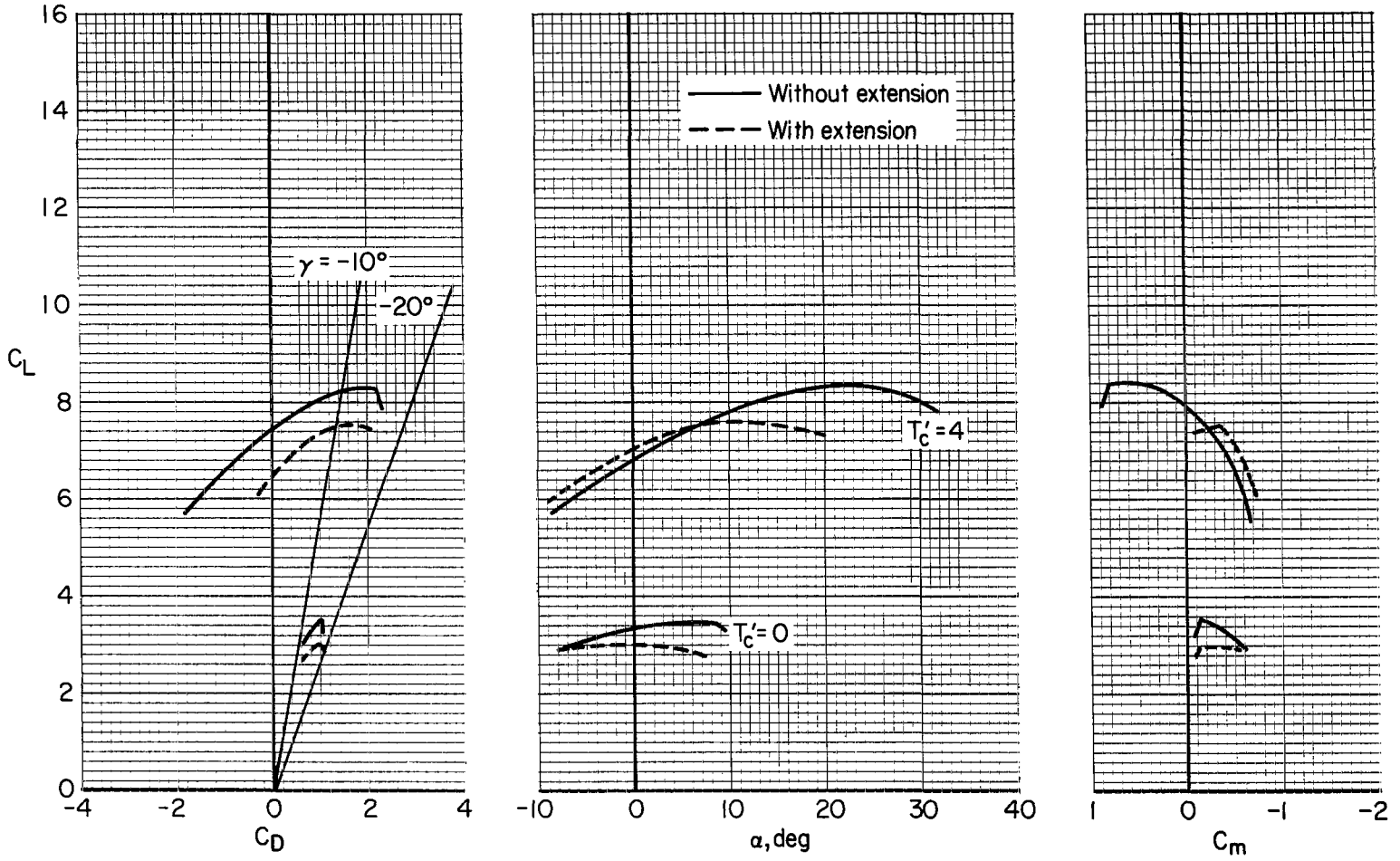

(b) Hinge 2.

Figure 18.- Concluded.

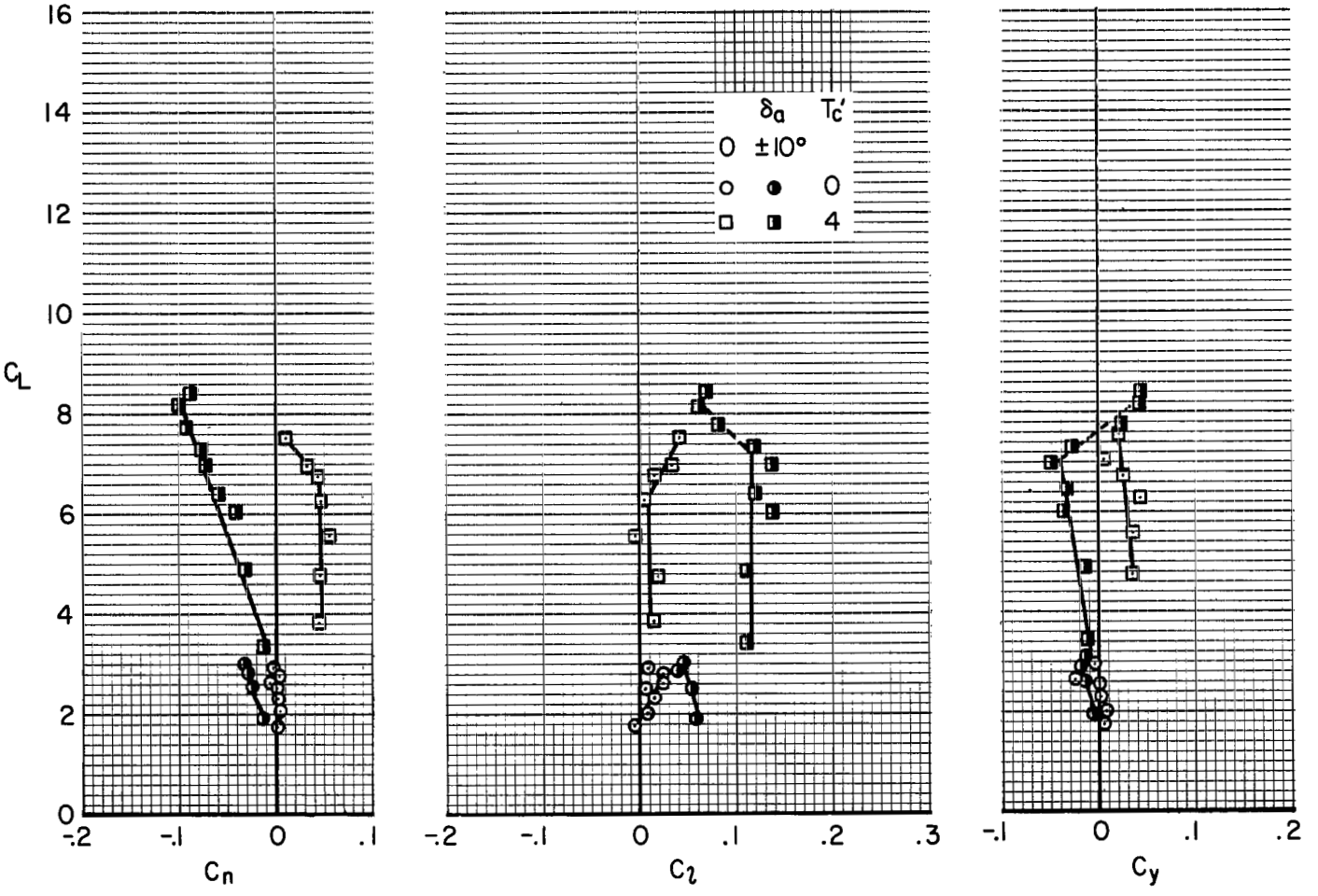

(a) Ailerons; $\delta_f = 40^\circ$, $\delta_A = 10^\circ$, U/V = 5.1.

Figure 19.- Lateral control effectiveness.

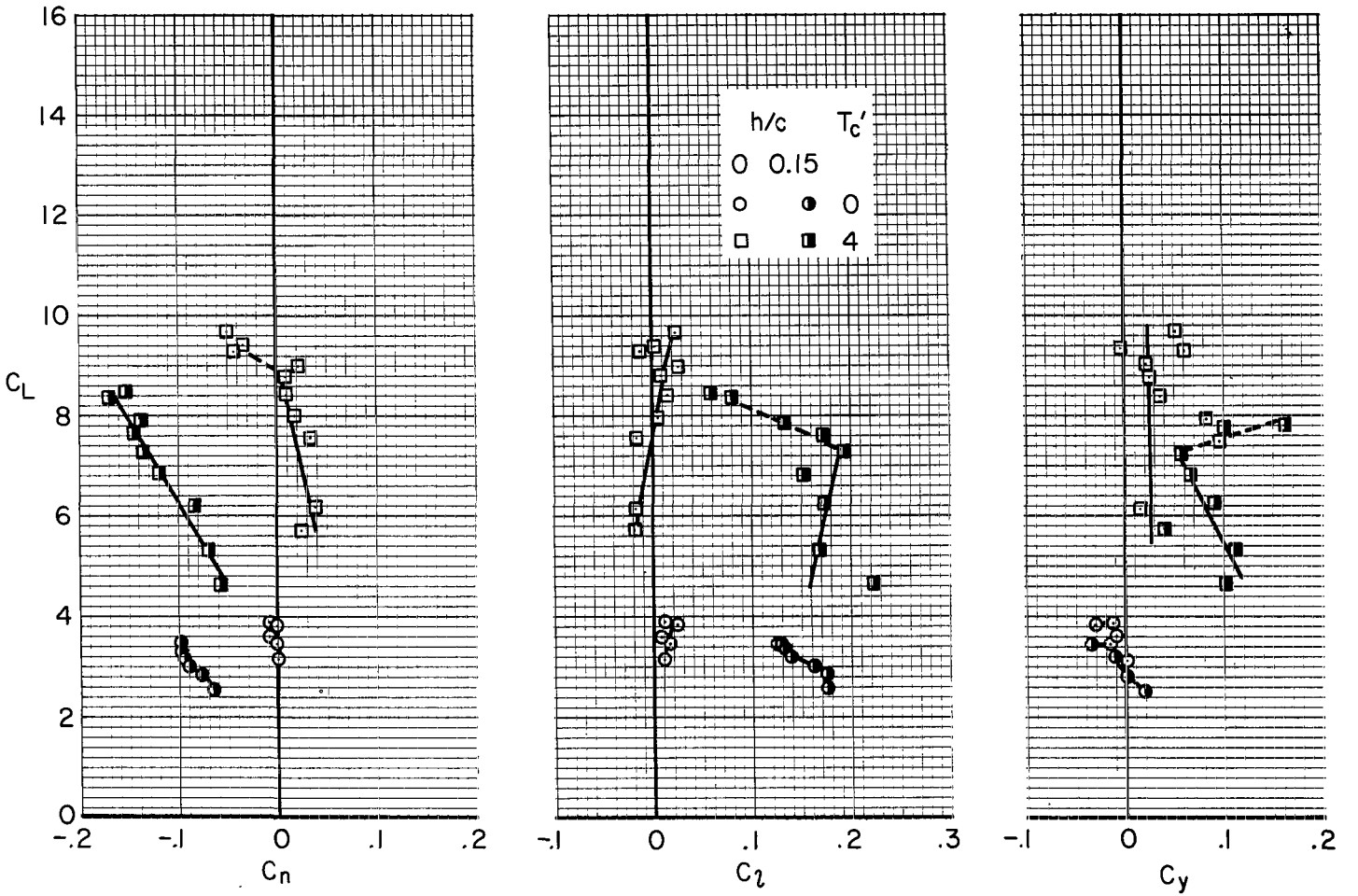

(b) Spoiler; $\delta_f = 70^\circ$, $\delta_A = 18^\circ$, slats on, U/V = 6.7.

Figure 19.- Concluded.

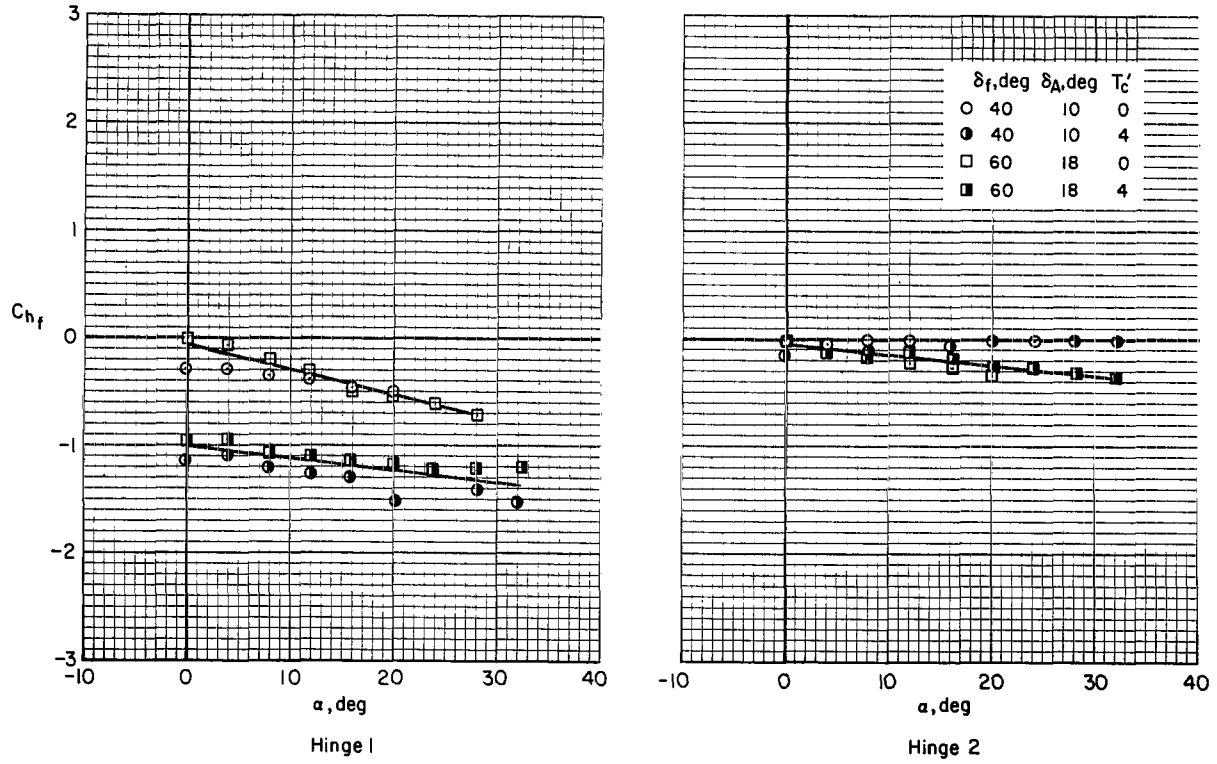

Figure 20.- Flap hinge moments.

"The aeronautical and space activities of the United States shall be conducted so as to contribute . . . to the expansion of human knowledge of phenomena in the atmosphere and space. The Administration shall provide for the widest practicable and appropriate dissemination of information concerning its activities and the results thereof."

—NATIONAL AERONAUTICS AND SPACE ACT OF 1958

NASA SCIENTIFIC AND TECHNICAL PUBLICATIONS

TECHNICAL REPORTS: Scientific and technical information considered important, complete, and a lasting contribution to existing knowledge.

TECHNICAL NOTES: Information less broad in scope but nevertheless of importance as a contribution to existing knowledge.

TECHNICAL MEMORANDUMS: Information receiving limited distribution because of preliminary data, security classification, or other reasons.

CONTRACTOR REPORTS: Scientific and technical information generated under a NASA contract or grant and considered an important contribution to existing knowledge.

TECHNICAL TRANSLATIONS: Information published in a foreign language considered to merit NASA distribution in English.

SPECIAL PUBLICATIONS: Information derived from or of value to NASA activities. Publications include conference proceedings, monographs, data compilations, handbooks, sourcebooks, and special bibliographies.

TECHNOLOGY UTILIZATION PUBLICATIONS: Information on technology used by NASA that may be of particular interest in commercial and other non-aerospace applications. Publications include Tech Briefs, Technology Utilization Reports and Notes, and Technology Surveys.

Details on the availability of these publications may be obtained from:

SCIENTIFIC AND TECHNICAL INFORMATION DIVISION

NATIONAL AERONAUTICS AND SPACE ADMINISTRATION

Washington, D.C. 20546